KEEP THIS COPY FOR REPRODUCTION PURPOSES

AD-A253 510

NTATION PAGE

Form Approved
OMB No. 0704-0188

1. AGENCY USE ONLY (Leave blank)	2. REPORT DATE	3. REPORT TYPE AND DATES COVERED
	May 26, 1992	Final Report, 1/15/89 - 1/14/92

4. TITLE AND SUBTITLE
The Interaction of UV-Laser Radiation with Metal and Semiconductor Surfaces

5. FUNDING NUMBERS
DAAL03-89-K-0028

6. AUTHOR(S)
Prof. Richard M. Osgood, Jr., Principal Investigator

7. PERFORMING ORGANIZATION NAME(S) AND ADDRESS(ES)
Columbia University
Microelectronics Sciences Laboratories
Mudd Bldg., Rm. 1322
New York, NY 10027

8. PERFORMING ORGANIZATION REPORT NUMBER

9. SPONSORING/MONITORING AGENCY NAME(S) AND ADDRESS(ES)
U. S. Army Research Office
P. O. Box 12211
Research Triangle Park, NC 27709-2211

10. SPONSORING/MONITORING AGENCY REPORT NUMBER
ARO 26223.2-PH

11. SUPPLEMENTARY NOTES
The view, opinions and/or findings contained in this report are those of the author(s) and should not be construed as an official Department of the Army position, policy, or decision, unless so designated by other documentation.

12a. DISTRIBUTION/AVAILABILITY STATEMENT
Approved for public release; distribution unlimited.

12b. DISTRIBUTION CODE

13. ABSTRACT *(Maximum 200 words)*

This report describes progress in a program to understand the fundamentals of UV laser interactions with solid surfaces. In the first, using the previously developed optical probes, we have made the first measurements of the surface photodissociation cross section, its yield, its wavelength dependence, and its dependence on surface conditions for two important metal-alkyl precursors. Second, we have successfully initiated a substantial new program in UV-laser photoemission for surface probing. This work has included establishing a new, tunable, two-photon photoemission apparatus including UHV chamber with an electron detection system, demonstration of a new technique to probe buried interfaces, the use of high-resolution, two-photon spectroscopy to probe surface-condition-dependent changes via image states, and the observation of space-charge-limited effects on surface photoionization spectroscopy.

14. SUBJECT TERMS
Metal-alkyls, Photodeposition, Laser photoemission, UV lasers, Two-photon photoemission, Single crystal copper, CaF_2, $Zn(CH_3)_2$ Excimer Laser.

15. NUMBER OF PAGES
79

16. PRICE CODE

17. SECURITY CLASSIFICATION OF REPORT	18. SECURITY CLASSIFICATION OF THIS PAGE	19. SECURITY CLASSIFICATION OF ABSTRACT	20. LIMITATION OF ABSTRACT
UNCLASSIFIED	UNCLASSIFIED	UNCLASSIFIED	UL

THE INTERACTION OF UV-LASER RADIATION WITH METAL AND SEMICONDUCTOR SURFACES

FINAL REPORT

R.M. Osgood, Jr.
Principal Investigator

January 15, 1989 through January 14, 1992

U.S. ARMY RESEARCH OFFICE

Contract #DAAL03-89-K-0028

Columbia University
Microelectronics Sciences Laboratories
New York, NY 10027-6699

APPROVED FOR PUBLIC RELEASE
DISTRIBUTION UNLIMITED

Submitted May 26, 1992

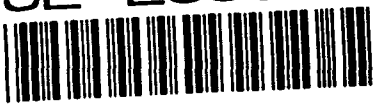

CONTENTS

A. STUDIES OF PHOTOELECTRON EMISSION FROM INTENSELY IRRADIATED SEMICONDUCTOR, METAL AND INSULATOR SURFACES

Our ARO program has allowed us to extend the use of high intensity laser photoemission techniques as well as to gain working knowledge of the physics of surfaces and interfaces under intense laser irradiation. Our progress has been in three areas, reported below in separate sections.

A1. Photoemission from Thick Overlying Layers of CaF_2 on Si(111)

Vacuum photoemission has been used extensively to probe the energy states of surfaces and near-surfaces regions of solids.[1] As overlayers are added to the surface, electron scattering reduces the electron yield and spectral information on the initial energy state of the transmitted electrons is lost. In such in instance, it might be felt that photoemissive measurements would be rendered useless. *In this section*, we show, however, that substantial photoyields can be obtained even from ultraviolet-illuminated semiconductor surfaces which are covered by thick insulating epitaxial layers. Further, we show that, by wavelength tuning of the light source, information can be obtained on electron transfer at the insulator-semiconductor interface, as well as the processes transporting electrons to the surface.

A1a. One-Photon Processes

In our experiments, we used the CaF_2/Si(111) materials system and an illumination source consisting of a tunable, pulsed ultraviolet laser. The CaF_2/Si(111) interface was selected

---

[1] M. Cardona and L. Ley, eds., *Topics in Applied Physics, vol. 26 (Spinger-Verlag, 1978).*

because it is a relatively well studied epitaxial system,[2,3] and because CaF_2 is transparent at the wavelengths used here. Further, because the valence-band maximum of silicon is located ~2.5 eV below the conduction band of calcium fluoride, internal photoemission into the insulating layer can be realized with a mid-ultraviolet light source. For our experiments, CaF_2 layers were deposited, by molecular-beam epitaxy, on *n*-type clean, reconstructed Si(111) (7×7) substrates with resistivities of 5-25 Ω.cm. The films quality was ascertained by transmission electron microscopy and Rutherford back-scattering. The samples were provided by Julia M. Phillips at AT&T Bell Laboratories. The samples were loaded in a separate ultra-high vacuum chamber (with a base pressure of 5×10^{-10} Torr) equipped with a heatable, rotatable manipulator and optical windows for the entrance and exit of the laser beam. The electron detection system consisted of a spherical-sector electrostatic energy analyzer with an energy resolution of about 150 meV. Emitted electrons were detected from a small solid angle (0.002 steradian) normal to the surface of the samples. Based on the measured sensitivity of our electron detection system, we estimated that we measure emitted electron fluxes as small as 10^3 electrons/pulse. The sample was biased to -5 Volts relative to the spectrometer to remove stray background electron emission and to reduce the effect of stray magnetic fields. Photons were provided by the frequency-doubled output of an excimer-pumped dye laser with 15 nanosecond pulse duration and tunable to a maximum photon energy of 4.6 eV. The laser beam was passed into the ultra-high vacuum chamber onto the sample, with an incidence angle of 67.5° and a spot size of about

---

[2] J.M. Phillips, *Mat. Res. Soc. Symp. Proc. 71, 97 (1986).*

[3] D. Rieger, F.J. Himpsel, U.O. Karlsson, F.R. McFeeley, J.F. Morar and J.A. Yarmoff, *Phys. Rev. Lett. 34, 7295 (1986).*

10^{-4} cm^2, and was allowed to exit the chamber without further reflection. It was found that the photoemission yield depended significantly on the initial preparation of the CaF_2 surface. In particular, without heat treating the sample, on chemically cleaned samples, no photoemission could be seen. Further, for a partially cleaned sample the signal was found to change during the laser exposure, with the magnitude of change dependent on the degree of sample cleaning. A careful study revealed that heating the sample to ~700° C for one hour allowed reproducible and stable results to be obtained, with a very small, ~10%, laser induced decay. The results of the treatment were investigated by separate experiments with a separate high resolution X-ray photoemission spectroscopy system. These measurements showed that the treatment removes adventitious carbon and oxygen (probably from CO_2 and H_2O). Note that the temperature of the heat treatment is moderate enough to prevent sublimation of CaF_2 molecules or loss of F surface atoms.[3] The initial experiments, which were made with 280-nm radiation, showed that photoemission could easily be seen from samples with overlayers up to the maximum thickness available ~8000 Å. Typical curves of energy-integrated photoemission signal versus laser intensity are shown in Figure 1 for 300- and 2000-Å CaF_2 films at 280 nm.

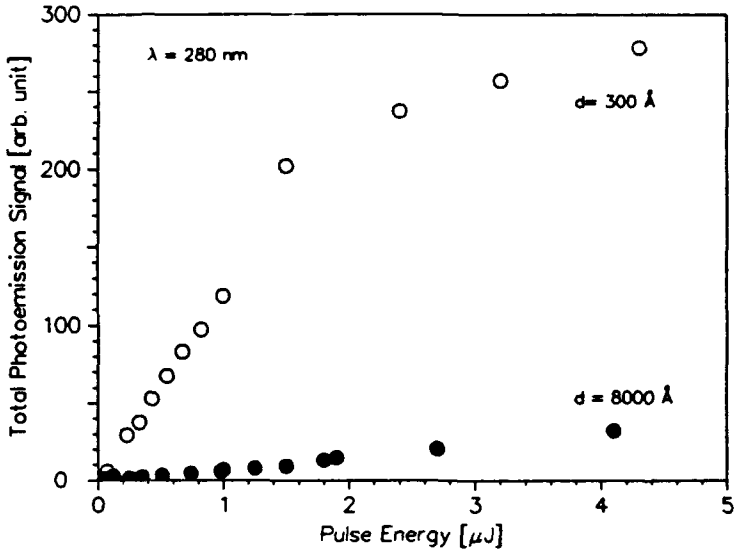

Figure 1 Energy-integrated photoemission signal *v.s.* laser pulse energy at λ=280 nm. CaF_2 thickness: closed circles d=8000 Å, open circles d=300 Å.

In each case, the curve exhibits an initial linear behavior with laser intensity. As the intensity is further raised, the photoemission becomes sublinear with intensity and then saturates. This saturation is tentatively ascribed to space-charge limitation of the emission outside of the insulator layer (see below). The reduction in space-charge effects for the thicker fluoride layers is consistent with the lower yields observed for larger fluoride layer thicknesses. In order to understand the origin of the photoelectron yield, determined as above, we measured yield as a function of photon energy. In obtaining this plot, we were careful to work at sufficiently low energy densities such that space-charge effects were not present. Figure 2 displays the resulting plot of the yield versus photon energy in the case of a CaF_2/Si(111) sample with a fluoride layer thickness d=300 Å. The curve can be approximately divided into two regions, 4.2-4.4 eV and 3.6-4.4 eV, corresponding to regimes exhibiting respectively stronger and weaker variation with photon energy. In the former case, as mentioned above, the yield varies linearly with energy density; in the latter case, even in the absence of space-charge effects, the yield varies as the square of the laser intensity. This behavior indicates that a single photon and a two-photon photoemission process are responsible for the photoemission in the two regimes, respectively. The data in Figure 2 can also be plotted as the cubic root of the yield versus photon energy. If this is done, see the inset in Figure 2, we find that the data from 4.2 to 4.5 eV may be extrapolated to intercept with the horizontal axis, to give a threshold value of 4.15 eV, while the

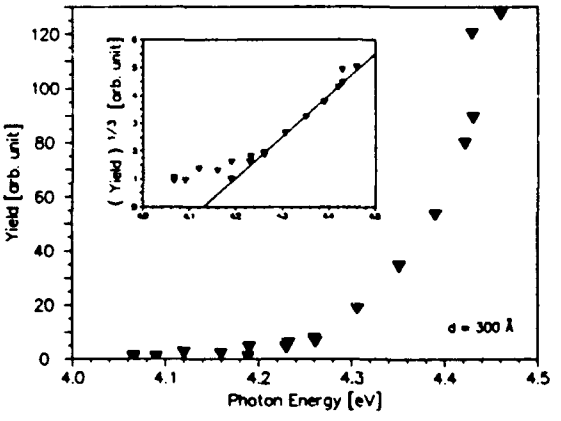

Figure 2 Plot of the photoemission yield *v.s.* the photon energy for a sample with a CaF_2 layer thickness of d=300 Å.

data from 3.6 to 4.2 eV extrapolate to e threshold of ~3.6 eV. An approximate estimate of the yield, in the linear portion of the curve, at a photon energy of 4.4 eV, shows it to be $\sim 10^{-6}$ electron/incident photon for a 300-Å thick fluoride. If we compare this value to the yield for emission from a clean Si surface into vacuum, at the same energy above threshold, as determined by F. Allen and G. Gobeli,[4] the estimated value is, for our case, two orders of magnitude lower. Considering that the electrons have to traverse a thick layer of CaF_2, this value seems quite reasonable. In order to determine the dependence of the photoemission on the thickness d of the fluoride layers, the yields from samples with different CaF_2 layer thicknesses were compared at a given photon energy and laser intensity, at room temperature. Figure 3 shows the photoemission yield, at $\lambda = 280$ nm, plotted against the CaF_2 layer thickness d. The yield decays exponentially with d, with a characteristic decay length of ~2600 Å. Finally, in order to gain information on the initial states of the photoemitted electrons, the electron energy distribution was measured as a function of the laser photon energy, fluoride thickness d and laser intensity. In general, the resulting electron energy distributions depended on the incident laser energy density. At high fluence, typically above 20 mJ/cm^2, the distributions were spread in electron kinetic energy and flattened, exhibiting a half width

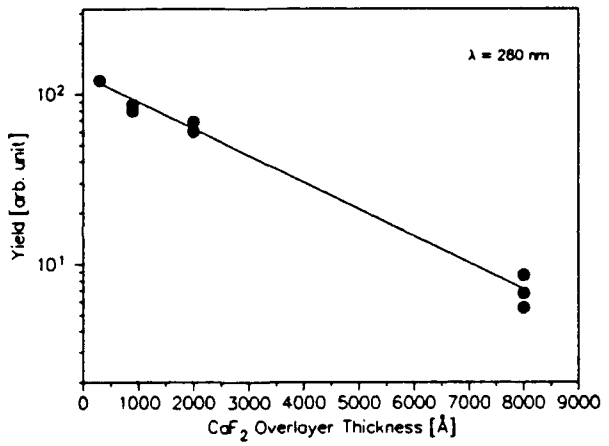

Figure 3 Semi-logarithmic plot of the photoemission yield versus the CaF_2 layer thickness, at $\lambda = 280$ nm.

---

[4] F. Allen and G. Gobeli, *Phys. Rev. 127, 150 (1962).*

approaching 1 eV (see Figure 4, for example). These results are indicative of space-charge broadening of the nascent electron energy distribution, an effect recently investigated by Gilton *et al.*[5] for pulsed photoemission from a metal surface. The saturation in the photoemission signal in Figure 1 is also attributed to this same space-charge effect. For thicker CaF_2 layers, the space-charge effect sets in at higher laser intensities. This is believed to be due to the lower photoemission yield for sample with thicker fluoride layers. For lower fluence, such as shown in Figure 4, the electron distribution narrows and assumes a constant shape characterized by a sharp rise near zero kinetic energy followed by an exponential decrease with increasing electron kinetic energy. Such a distribution has been observed in other laser photoemission experiments.[6] In this low-fluence region, the yield increases linearly with intensity (see Figure 1); however, the "temperature" of the distribution, as determined by a Boltzmann fit to the exponential tail was sensitive to fluence. At the lowest fluence at which reliable data could be obtained, ~1 mJ/cm^2, the fitted temperature approached that of the lattice, i.e. 550 °C ± 100 °C versus 300 °C for room temperature. In general, the measurements showed only an extremely weak dependence of the distribution, if any, on photon

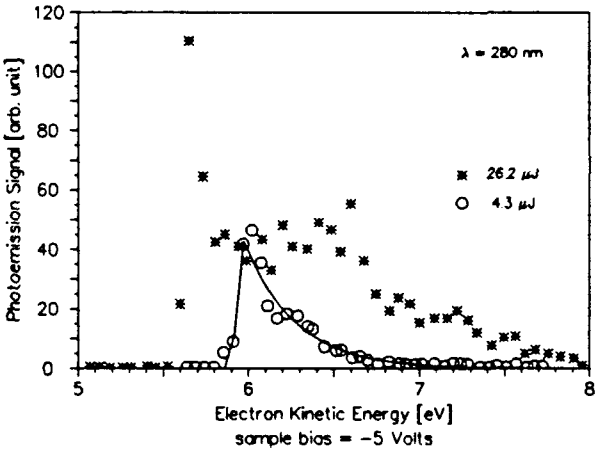

Figure 4 Photoemission signal *vs.* electron kinetic energy, for a CaF_2 layer thickness d = 300 Å. Laser pulse energy: stars 2.62 mJ, circles 0.43 mJ.

---

[5] T. Gilton, J.P. Cowin, G. Kubiak and A.V. Hamza, *J. Appl. Phys. 68, 1 (1990).*

[6] S. Schuppler, N. Fisher, Th. Fauster and W. Steinmann, *Appl. Phys. A 51, 322 (1990).*

energy. For example, as the photon energy was tuned from ~4.1 to 4.6 eV, no significant change in the distribution could be discerned, even at the lowest laser fluence. The data and results obtained above are consistent with a photoemission process which is initiated by a photoexcitation in the valence band of Si from energy levels near $\Gamma_{25'}$ along Λ_3 to energy levels near $\Gamma_{2'}$ along Λ_1 (the transition near $\Gamma_{25'} \rightarrow \Gamma_{2'}$ is close to our threshold for single photon process[7]). On their way to the interface, the electrons relaxed to the bottom of the energy band containing $\Gamma_{2'}$ before entering into the conduction band of the overlying CaF_2 film. Since the $\Gamma_{2'}$ point is ~ 0.55 eV above the conduction band,[8,3,9] the electrons will undergo further energy relaxation upon entering the CaF_2 crystal. After traversing the film they will be emitted into the vacuum. Direct vacuum emission is possible since, according to recent calculations,[10,11] the electron affinity of CaF_2 is negative by a few tens of an eV. As a result, the electrons injected into CaF_2 can still be emitted into vacuum, even if they are relaxed to the conduction band bottom of CaF_2. The increase in the "temperature" of the electron distribution with the number of emitted electrons is expected from the Columbic repulsive forces among these electrons. The fact that the apparent positions of the lowest energy electrons shift monotonically to lower energies as the distribution broadens, as is seen in a series of

---

[7] J. C. Phillips, *Solid State Physics, 18, 56 (1966).*

[8] O. Madelung, M. Schulz and H. Weiss, eds., *Landolt-Börnstein, Semiconductors, vol. 17, (Springer-Verlag, Berlin, 1982).*

[9] R. Mamy, B. Carricaburu, A. Munoz-Yague and C. Fontaine, *Surf. Sci. 222, 119 (1989).*

[10] J. Morrar, *private communication.*

[11] R.T. Poole, D.R. Williams, J.D. Riley, J.G. Jenkin, J. Liesegang and R.C.G. Leckey, *Chem. Phys. Lett. 36, 401 (1975).*

experiments not described here, indicates that the space charge effects are occurring outside of the sample.

The power law dependence of the yield on photon energy above the threshold has been theoretically established for internal photoemission,[12] as well as for photoemission from bare semiconductor surfaces,[13] yielding power values varying from 1 to 2.5, corresponding to different excitation and scattering processes. However, as reported above, a cubic dependence is found to best fit our experimental data.[14] While our study of the lower photon-energy threshold process is not as complete, its onset at approximately 3.6 eV is consistent with the transitions $\Lambda_3 \rightarrow \Lambda_1$ ($\Gamma_{25'} \rightarrow \Gamma_{15}$) and requires the second photon to access states above the CaF_2 conduction band. Note that the two-photon event may be a simultaneous or sequential process.

In conclusion, we have observed low-energy photoemission through very thick, 8000 Å, epitaxial layers. We have found that significant transfer occurs only after direct pumping of the bulk $\Gamma_{2'}$ Si band. Clearly this same technique can be extended to map out other excited, buried interfacial or bulk bands by single or two photon techniques. Finally, although not discussed in this report, we have recently found[15] an analogous behavior for the SiO_2/Si(111) system. This result shows that the phenomenon is quite general to wide band gap insulator systems on semiconductors.

---

[12] J.S. Helman and F. Sanchez-Sinencio, *Phys.Rev. B 7, 3702 (1973).*

[13] E. O. Kane, *Phys. Rev. 127, 131 (1962).*

[14] G.W. Gobeli and F. G. Allen in *Semiconductors and Semi-metals, ed. R.K. Williamson and A. C. Beer, vol. 2, p. 263 (Academic Press, 1986).*

[15] B. Quiniou, W. Schwarz, Z. Wu amd R.M. Osgood, Jr., *unpublished.*

A1b. CaF_2/Si(111) Interfacial State: a Two-Photon Photoemission Study

We reported above internal photoemission in silicon at a Si(111)/CaF_2 interface and significant electron emission in vacuum at the CaF_2/vacuum interface subsequent to electronic transport in the CaF_2 conduction band through CaF_2 epitaxial layers up to 8000 Å thick[16].

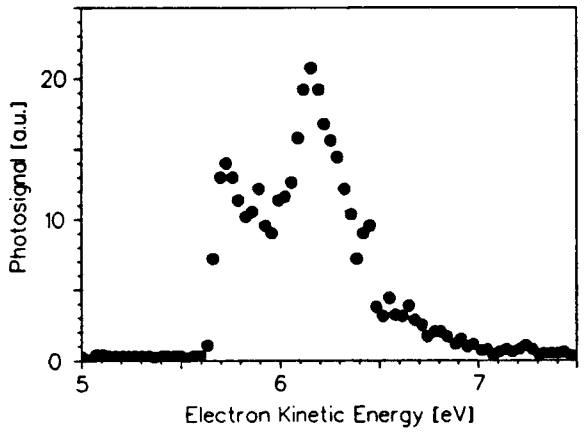

Figure 5 Photoelectron EDC from a CaF_2(500 Å)/Si(111) sample excited with 2.41 eV incident photons.

To further demonstrate the usefulness and the specificity of our new technique, we decided to investigate an interfacial state at the same Si(111)/CaF_2 interface. This interfacial state was suggested by several authors[17] and clear experimental evidence of its existence was given by T.F. Heinz *et al.*[18]. These latter authors used non-destructive second harmonic generation (SHG) and sum frequency generation (SFG) techniques to determine the characteristics of this interfacial state. This state offers attractive features, one of which being its location in the energy gap at the interface, above the Fermi level. Not being resonant with any bulk or interface energy features in Si or in CaF_2, the state is anticipated to have a specific signature

---

[16] B. Quiniou, W. Schwarz, Z. Wu, R.M. Osgood, Jr., Q. Yang and J.M. Phillips, *Appl. Phys. Lett. 60, 183 (1992).*

[17] F.J. Himpsel, U.O. Karlsson, J.F. Morar, D. Rieger and J.A. Yarmoff, *Phys. Rev. Lett. 56, 1497 (1986)* and D. Rieger, F.J. Himpsel, U.O. Karlsson, F.R. McFeely, J.F. Morar and J.A. Yarmoff, *Phys. Rev. B 34, 7295 (1986).*

[18] T.F. Heinz, F.J. Himpsel, E. Palange and E. Burstein, *Phys. Rev. Lett. 63, 644 (1989)* and E. Palange, T.F. Heinz, F.J. Himpsel and E. Burstein, *Bull. Am. Phys. Soc. 33, 298 (1988).*

in our photoemission measurements. Furthermore, the fact that the state is located above the Fermi level, *i.e.* it is normally empty, is also interesting to us to the extend that it will allow us to combine our probing technique with a two-photon photoemission process. In other words, a first photon would excite an electron to this interfacial state and a second photon would be required to internally photoemit the electron to the CaF_2 conduction band. The experimental procedures as well as the experimental set-up which we used to carry out our experiments were also in the previous section (**A1a**). A typical energy distribution curve, obtained with an incident photon energy $\hbar\omega$=2.41 eV on a Si(111)/CaF_2 sample with a 500 Å thick CaF_2 layer, is shown in Figure 5 (the electron energy distribution curve has been corrected neither for the sample bias, -5 Volts, nor for the spectrometer contact potential). It exhibits two distinct features. The first low energy peak is assumed to originate from electrons photoemitted in Si and having relaxed to the bottom of the conduction band in Si before being transported through the CaF_2 layer and ejected into vacuum (such a peak was observed in our previous studies, see section **A1a**). The higher energy electrons, appearing in the second peak, are believe to have been emitted from the initially empty interfacial state. Further study will be necessary to ascertain unambiguously our claim. Nevertheless, two-photon photoemission processes are clearly responsible for the emission observed in Figure 5, *i.e.* for the two peaks in the electron energy distribution curve. This is shown, for instance, in Figure 6, where the amplitude of the peak at 5.8 eV is plotted against

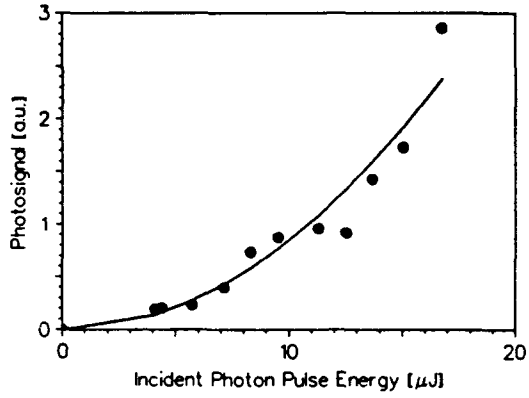

Figure 6 Photosignal from a CaF_2(500 Å)/Si(111) sample versus incident pulse energy (2 mm. spot size)

the incident laser intensity, for a given photon energy $\hbar\omega$=2.4 eV. It is also important to study how the observed emission is modified upon changes in the exciting photon energy. Figure 7 shows how the photosignal, at the given electron kinetic energy of 6.2 eV, varies with the incident photon energy $\hbar\omega$, while the photon intensity is kept constant. The obvious observation is that a strong resonance occurs for a photon energy of about 2.43 eV. This value is in excellent agreement with the value reported by T.F. Heinz *et al.*[18] for the energy separation, 2.4 eV, between this empty anti-bonding interfacial state and its occupied bonding counterpart. The experimental width of this resonance, roughly 0.2 eV, is believe to reflect inelastic scattering of the emitted electron rather than any intrinsic property of the interfacial electronic state. In conclusion, we further demonstrated the scope of photoemission through epitaxial insulator layer on semiconductors for the probing of buried interfaces. In addition, this technique is shown to be complementary to SHG and SFG. Indeed, for these latter to be operational it is required for the overlayer to be transparent to both the fundamental incident radiation ω and its second harmonic 2ω (or $\omega+\omega'$). For the harmonic or sum frequency signal to be generated, it is also necessary that a symmetry disruption in the lattices symmetries occurs at the interface (which is not necessarily the case for epitaxial materials, *e.g.* GaAs/AlGaAs). These restrictions do not apply to our photoemission technique.

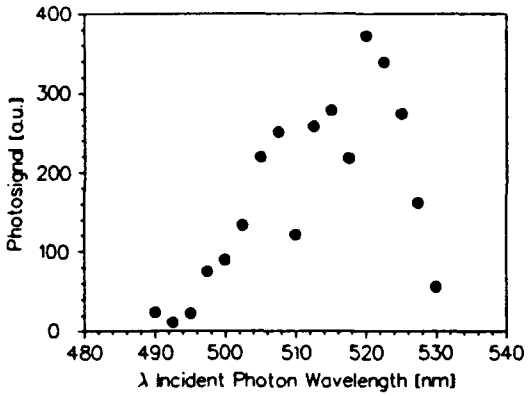

Figure 7 Photosignal from a CaF_2(500 Å)/Si(111) sample versus incident photon wavelength.

More effort will be required to complete this preliminary study; this is scheduled to occur in the near future.

A2. Image-Potential Induced States on Copper Surfaces

A2a. Temperature and Adsorption Dependence of Image-Potential Induced States on Cu(100)

We report significant results in a systematic study of the dependence of image-potential states on surface temperature and oxygen adsorption on Cu(100) surface using two-photon photoemission spectroscopy. Image-potential states are unique surface (actually near-surface) states with very narrow energy widths (a few tens of meV[19,20]). They are bound states between the image potential and the surface barriers. Like the hydrogen atom, the image-potential states form Rydberg progressions, with n=1 state having about 0.5 - 0.8 eV binding energy for most of the metal surfaces which have been studied.[21] Since these image states are normally unoccupied, inverse photoemission spectroscopy[22,23,24,25] and two-photon photoemission spectroscopy[26,27] have been used to investigate these image states, although only the latter method offers measurement resolution comparable to the actual lifetime-limited width. Because of this resolution, two-photon photoemission spectroscopy allows the use of

---

[19] P.M. Echenique, F. Flores and F. Sols, *Phys. Rev. Lett. 55, 2348 (1985).*

[20] S. Schuppler, N. Fisher, Th. Fauster and W. Steinmann, *Appl. Phys. A 51, 322 (1990).*

[21] W. Steinmann, *Appl. Phys. A 49, 365 (1989)* and references therein.

[22] S.L. Hubert, P.D. Johnson, N.G. Stoffel, W.A. Royer and N.V. Smith, *Phys. Rev. B 31, 6815 (1985).*

[23] A. Goldmann, V. Dose and G. Borstel, *Phys. Rev. B 32, 1971 (1985).*

[24] G. Borstel and G. Thorner, *Surf. Sci. Rep. 8, 1 (1987).*

[25] D. Straub and F.J. Himpsel, *Phys. Rev. B 33, 2256 (1986).*

[26] K. Giesen, F. Hage, F.J. Himpsel, H.J. Riess and W. Steinmann, *Phys. Rev. B 35, 971 (1987).*

[27] R.W. Schoenlein, J.G. Fujimoto, G.L. Esley and T.W. Capehart, *Phys. Rev. B 43, 4688 (1991).*

slight shifts in the image state to probe surface conditions, such as surface adsorption or temperature.

Our two-photon photoelectron spectroscopy set-up and the attached ultra-high vacuum system were described in detail earlier in section **A1a.**

In selecting a copper surface for our study, we initially considered Cu(111) because of its well known resonant enhancement using two-photon excitation.[21] However, this enhancement results from the excitation from a narrow occupied surface state just below the Fermi level, E_f, thus any measurement of the temperature dependence of the two-photon signal will reflect thermal alteration of both the surface state and the image-potential state. In fact, previous observations have shown that the resonantly enhanced image state photoemission on Cu(111) is strongly quenched at the relatively low temperature of 200 °C.[28] In order to study the properties of image states without being affected by surface states, we chose the Cu(100) surface, in which there is no occupied surface state just below E_f so that the image states would be populated only by non-resonant excitation from the bulk states. In our experiments, the (100) surface of a copper (99.999 % purity) single crystal was chemically cleaned before being loaded into an ultra high vacuum chamber. The sample was then sputtered and annealed (~ 850 K) until a sharp (1 × 1) low-energy electron diffraction pattern appeared. A typical photoemission signal with exciting photon energy 4.55 eV is shown in Figure 8, in which the electron energy distribution curve (EDC) is shifted by 5 eV due to the -5 Volt bias. The large peak at ~ 5 eV is due to single-photon photoemission from the tail of the Fermi distribution[20]. An expanded

---

[28] K. Giesen, F. Hage, F.J. Himpsel, H.J. Riess and W. Steinmann, *Phys. Rev. Lett. 55, 300 (1985).*

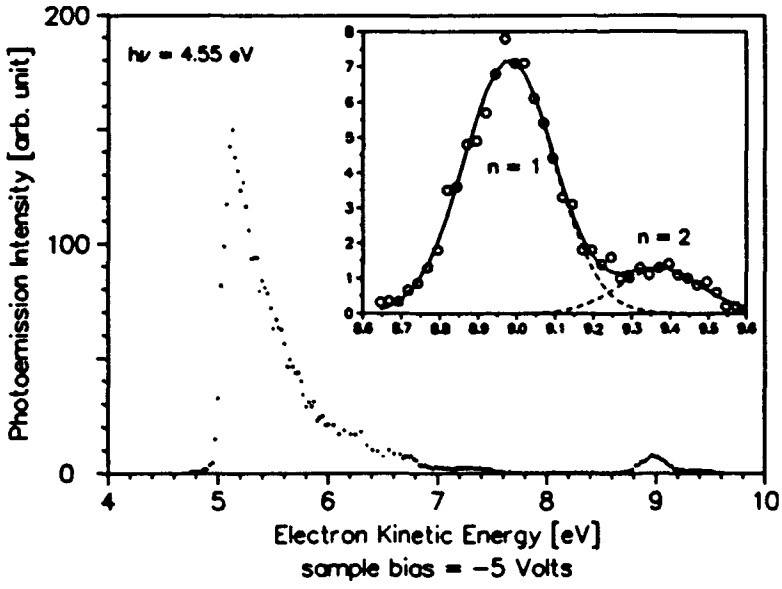

Figure 8 Photoemission signal from Cu(100) with an incident photon energy of 4.55 eV.

view of the image-potential state signal around 9 eV is shown in the inset of Figure 8, where the two peaks correspond to the hydrogenic image-potential states n=1 and n=2, respectively, as were first seen by Giesen *et al*[26]. Shown in Figure 9 is the temperature dependence of the n=1 image-potential peak position. It is important to emphasize that the data in Figure 9 were taken with the integrated area of the first low energy peak (see Figure 8) held constant by adjustment of the incident laser flux. This step was necessary since it was found that the image peak position was affected not only directly by temperature but also by the space charge created by the large low-energy electron peak. While space charge broadening of the electron energy distribution curves has been reported by several groups[29,30,31], there has not been a previous discussion of the fact that the energy position of photoemission peaks can be easily shifted due to the presence of high electron densities in other features, a phenomenon of particular importance in pulsed-laser photoemission

---

[29] T.L. Gilton, J.P. Cowin, G.D. Kubiak and A.V. Hamza, *J. Appl. Phys. 68, 4802 (1990).*

[30] K. Giesen, F. Hage and W. Steinmann, *Ann. Isr. Phys. Soc. 6, 446 (1984).*

[31] A.V. Hamza and G.D. Kubiak, *J. Vac. Sci. Technol. A 8, 2687 (1990).*

experiments. In our case, the space charge and temperature variation shift the image peak position in opposite directions. However, by keeping the total number of low-energy electrons constant, the shift due to the space charge was kept constant and we were able to observe the direct variation in the peak position with temperature. A linear fit to the data in Figure 9 yielded the rate of change in kinetic energy with temperature $\Delta E_K/\Delta T = -(2.5\pm0.7) \times 10^{-4}$ eV/K. The experimental uncertainty was mainly due to the fluctuation in the laser flux. According to the calculation of Herzfeld,[32] the slope of the work function variation with temperature for Cu is $\Delta\phi/\Delta T = -2.5 \times 10^{-4}$ eV/K. Using $\Delta E_K = \Delta\phi - \Delta E_b$, with E_b being the binding energy of the image state, we conclude that, within our experimental uncertainty, the binding energy E_b of the n=1 image-potential state is insensitive to the temperature variation within the temperature range 300 K - 715 K. In other words, the image-potential state n=1 is pinned to the vacuum level. In view of the fact that the available experimental data on the temperature dependence of work function are surprisingly scarce, it is interesting to note that the data such as shown in Figure 9 provides an interesting method to measure the temperature dependence of work function on certain clean metal surfaces. This

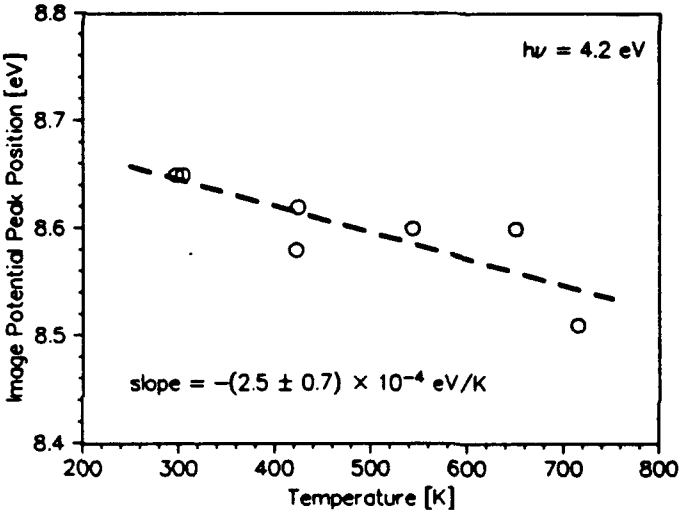

Figure 9 Variation of the n=1 image-potential peak position with temperature.

[32] K.F. Herzfeld, *Phys. Rev. 35, 248 (1935)*. Temperature dependence of work function on a selected number of metals has recently been calculated by A. Kiejna *Surf. Sci. 178, 349 (1986)*. The calculated value for Cu(100) is -1.5 × 10^{-4} eV/K.

method is expected to have advantages over the conventional technique of fitting the photoelectric yield near threshold to a Fowler plot. In order to cross check the above measurement of the pinning of the image state to the vacuum level, we measured the shift in the n=1 image state after exposing the Cu(100) surface to oxygen since it is well known that oxygen adsorption increases the work function on Cu surfaces, *i.e.* moves the vacuum level upward. Note that the effect of oxygen adsorption on Cu(111) was studied by Rieger *et al.*[33] However, in that case, no shift in the image peak could be observed since the resonant image-potential state signal disappeared upon the adsorption of oxygen (1000 L). In our experiments, the exposure to the oxygen gas was done by back-filling the chamber with research grade O_2, while the sample was at room temperature. Shown in Figure 10 are the image peaks for clean and 1.5 L O_2 exposed Cu(100). The image state signal was reduced after the exposure to O_2. A shift in the image peak position by ~ 0.07 eV, towards higher kinetic energy, can be clearly seen. Both the direction and the magnitude of the shift are consistent with the increase of work function after the exposure to oxygen.[34] Our temperature-dependent shift data as well as the oxygen adsorption data are consistent with the phase analysis model.[35,36,37] According to this model, the binding energy of the n=1 image state is determined from the Bohr-like quantization condition : $\phi_B + \phi_C = 2\pi$. Here ϕ_B and ϕ_C are respectively the phase changes of the electron at the image-potential and the surface barriers as it is reflected back and forth

---

[33] D. Rieger, T. Wegehaupt and W. Steinmann, *Phys. Rev. Lett. 58, 1135 (1985).*

[34] A. Spitzer and H. Lüth, *Surf. Sci. 118, 121 (1982).*

[35] N.V. Smith, *Phys. Rev. B 32, 3549 (1985)* and *Rep. Prog. Phys. 51, 1227 (1988).*

[36] E.G. McRae, *Rev. Mod. Phys. 51, 541 (1979).*

[37] P.M. Echenique and J.B. Pendry, *J. Phys. C 11, 2065 (1978).*

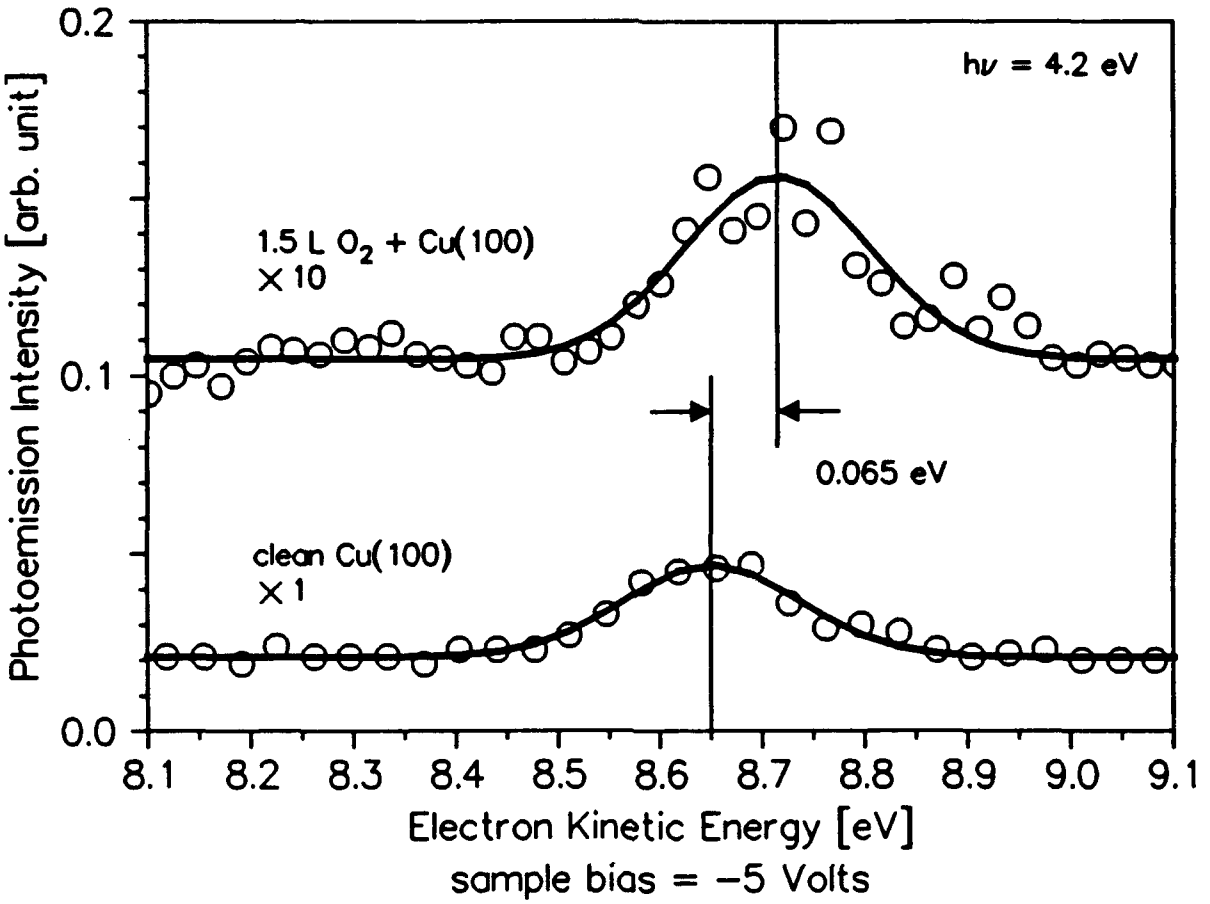

Figure 10 Image-potential peak position before and after 1.5 L oxygen-gas exposure.

between these two potential barriers. The value of ϕ_B is given by $\phi_B=[(3.4\ \text{eV})/(E_{vac}-E)]^{1/2}\pi-\pi$, where E_{vac} is the vacuum energy level and E the electron energy. The value of ϕ_C depends on the energy band structure on Cu(100). Assuming that the only effect of oxygen adsorption is to shift the vacuum level upward with respect to the Fermi level, the phase model predicts that the n=1 level shifts upward by the same amount as the vacuum level does, which is consistent with what is observed. However, when the surface temperature is raised, a small change occurs in the barrier at the crystal surface. In particular, according to

the measurement by Knapp *et al*,[38] the temperature coefficient for the bulk energy bands of Cu is of the order of 10^{-4} eV/K. This shift in the energy bands causes a change in ϕ_C, the magnitude of which is given by :

$$\Delta\phi_C \approx \frac{\pi}{E_{X_1} - E_{X_4'}} \times 10^{-4}\ eV/K \approx 5 \times 10^{-5}\ rad/K\ .$$

Here we have used $E_{X_1} - E_{X_4'} = 6.1$ eV. The change in binding energy is given by :

$$\Delta(E_{vac} - E) = -\frac{2(E_{vac} - E)^{3/2}}{\pi\sqrt{3.4}}\Delta\phi_B\ .$$

Noting that $|\Delta\phi_B| = |\Delta\phi_C|$ and that the binding energy of the n=1 image state at room temperature is 0.55 eV, we find that the change in binding energy is of the order of 10^{-5} eV/K, which is indeed quite small for our temperature range. While the temperature dependence of the image peak position yields information about the binding energy of the image state, the temperature dependence of the amplitude of the image peak provides important insight into the dynamic properties of the image state. Since the image state interacts only weakly with the crystal, one would expect a weak temperature

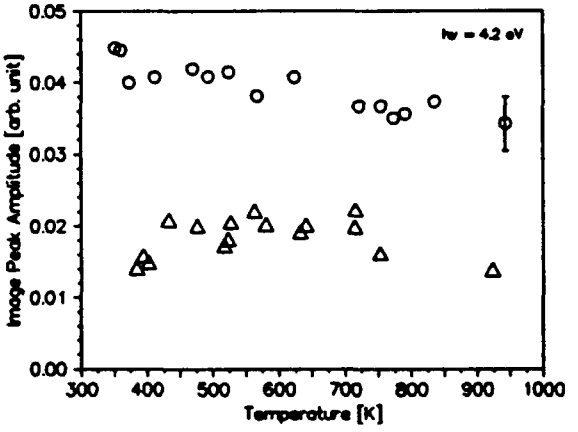

Figure 11 Dependence of the image-potential peak amplitude with temperature (see text).

[38] J.A. Knapp, F.J. Himpsel, A.R. Williams and D.E. Eastman, *Phys. Rev. B 19, 2844 (1979).*

dependence of the image peak amplitude. This weak temperature dependence was first observed using inverse photoemission. The results of our two-photon photoemission study confirmed this observation, as can be seen from the data shown in Figure 11. In order to discriminate between the change due to temperature and to spurious surface changes as a result of chemical reactions such as oxidation, the temperature was cyclically varied between 300 K and 1000 K. The data points represented by open triangles were taken after the sample was heated to ~ 1000 K (~ 150 K above the annealing temperature) for a few minutes. Apparently, some permanent change in the surface condition occurred during the high-temperature treatment. It is, however, interesting to note that the temperature dependence of the image peak amplitude is as weak on the modified surface as on the clean Cu(100) surface. The modification of the surface condition could be due to (1) surface disordering or (2) the segregation of sulfur to the surface[39] at high temperature (~ 1000 K). The first possibility, *i.e.* surface disordering, was ruled out based on the observation that the Cu(100) surface does not lose order even for temperatures as high as 1273 K.[40] In this connection, it would be interesting to study image-state photoemission from a Cu(110) surface, which was reported to exhibit strong surface disordering at temperatures as low as ~ 600 K. No such study has been reported yet. The sulfur segregation hypothesis seems to agree with the observation that after the high temperature treatment the position of the image peak is found to shift to higher kinetic energy by ~ 0.07 eV, indicating a change in the work function of the surface. Like oxygen, the sulfur atoms which have segregated to the surface are also expected to reduce the image peak amplitude. The fact that the same weak temperature

---

[39] S. Thevuthasan and W.N. Unertl, *Appl. Phys. A 51, 216 (1990).*

[40] D. Gorse and J. Lapujoulade, *Surf. Sci. 162, 847 (1985).*

dependence persisted on the sulfur-modified surface seems to indicate that the image-state electrons are still decoupled from this surface, even in the presence of adsorbates.

In conclusion, by using two-photon photoelectron spectroscopy, we confirmed and strengthened the observations of previous studies using inverse photoemission spectroscopy. The image-potential state is pinned to the vacuum level and the image peak amplitude depends very weakly on the sample temperature. A new method of measuring the temperature dependence of work function was suggested. This method consists of measuring the kinetic energy of image state photoelectrons while keeping the space charge fixed. Both the temperature and oxygen adsorption change the work function of copper and consequently the kinetic energy of image-state photoelectrons. However, whereas the temperature does not affect the image-state peak amplitude, oxygen adsorption drastically reduces the image-peak amplitude. This same phenomena was observed on a Cu(100) surface modified by high-temperature heating. This modification was believed to be due to sulfur segregation to the surface. These observations seem to indicate that the unshielded charges on the adsorbed O or S atoms act as strong scattering centers for the image-state electrons.

A2b. A Consequence of the Pinning of Image-Potential Induced States to the Vacuum Energy Levels: Temperature Variation of Surface-Plasmon Frequencies for Transition Metal Surfaces

In the previous section we reported the results of our work on image-potential induced states at the (100) crystallographic face of copper. We showed that the binding energies E_B of image-potential states are independent of temperature and adsorption, *i.e.* we demonstrated the pinning of image-potential induced states to the vacuum level. We extended this result to

understand the behavior of surface plasmons (these surface electronic excitations are closely connected to the image potential) upon temperature changes. In the framework of a simple model for the (electron/surface) interaction,[41] the independence of the image-potential states binding energies E_B upon temperature variation, *i.e.* $\Delta E_B/\Delta T=0$, leads to:

$$(1) \qquad \frac{\Delta}{\Delta T}\left(\frac{N}{\omega_s^{\,2}}\right) = 0 \quad ,$$

where N is the free electron density and $\omega_s=\omega_s(\kappa=0)$ is the $\kappa=0$-eigenfrequency of the surface plasmon. Introducing the linear expansion temperature coefficient α, we obtain:

$$(2) \qquad \frac{\Delta \omega_s}{\Delta T} = -\frac{3}{2}\alpha\,\omega_s \quad .$$

This results, trivial for a free-electron like metal, is shown to apply to the more complex transition metals. Equation 2 is therefore also obeyed by d-band transition metals, for which the surface-plasmon eigen frequency is shifted from a free-electron value, due to interband transitions. To our knowledge, the temperature dependence of the $\omega_s(\kappa=0)$ eigenfrequency of surface plasmons on the (100) face of Cu has not been measured yet, but this measurement was carried out recently by M. Rocca *et al.*[42] for Ag(100). They experimentally found that the rate of change of $\omega_s(\kappa=0)$ with temperature is linear and given by: $\Delta\omega_s/\Delta T = -(8.9\pm0.9)\times10^{-5}$ eV/K. This experimental value for $\Delta\omega_s/\Delta T$ is to be compared to the value which can be

---

[41] A.Zangwill, *Physics at Surfaces, p. 141-144 (Cambridge University Press, 1989).*

[42] M.Rocca, F. Moresco and U. Valbusa, *Phys. Rev. B 45, 1399 (1992).*

retrieved from Equation 2, with[43] $\alpha = 19\times10^{-6}$ K^{-1} and $\omega_s \approx 3.69$ eV[42]: $\Delta\omega_s/\Delta T = -10.5\times10^{-5}$ eV/K. The agreement between these two values is good and suggest a wide scope for the validity of Equation 2. This result can be ascertained by a wide range of experiments (high resolution EELS, laser Raman spectroscopy, *etc.*). For instance, it would be particularly interesting to study the multiple plasmon and surface plasmon satellites of a core state emission in the "shake-up" portion of an XPS spectrum: upon a temperature variation ΔT, the variation $n\Delta\omega_s$ of the energy loss corresponding to a n-surface plasmon process would, for n sufficiently large, become larger than the limited energy resolution of an XPS spectrometer.

A2c. Resonant Image-Potential Induced States on Cu(110)

Although the existence of an energy gap at the vacuum energy level was originally thought to be necessary in order to observe image-potential induced states at the surfaces of metals, we have succeeded in observing and resolving the image-potential states at the (110) crystallographic face of copper. On Cu(110), these states are resonant with bulk Bloch states. A sample of our experimental results is given in the electron energy distribution curve (EDC) shown below in Figure 12. This electron energy distribution curve was obtained by two-photon photoemission from a Cu(110) surface excited by 4.16 eV photon and for a sample bias of -5 Volts. The experimental widths of the n=1 and n=2 peaks, respectively ~ 0.35 and ~ 0.25 eV, are not limited by the apparatus resolution: ~ 0.20 eV. The widths of the resonant image-potential state peaks are about an order of magnitude larger than the typical widths of non-

[43] R.C. Weast, ed., *Handbook of Chemistry and Physics, p. D-185 (CRC Press, 1986).*

resonant image-potential induced state peaks.[44] The increased broadening of the resonant image-potential states as they move closer to the surface, *i.e.* from n=2 to n=1, is not surprising. This phenomenon is, in fact, well known in quantum physics and arises from the increased coupling of a discrete energy level (the image-potential state) with an energy continuum (the bulk Bloch states). This is, for example, analogous to the broadening of the discrete energy levels of an atom upon adsorption, where the broadening increases as the (atom/surface) distance decreases.[45] More thorough investigation of this phenomenon is on the way. For instance, we are currently carrying out experiments to determine the effective masses of such resonant image-potential states.

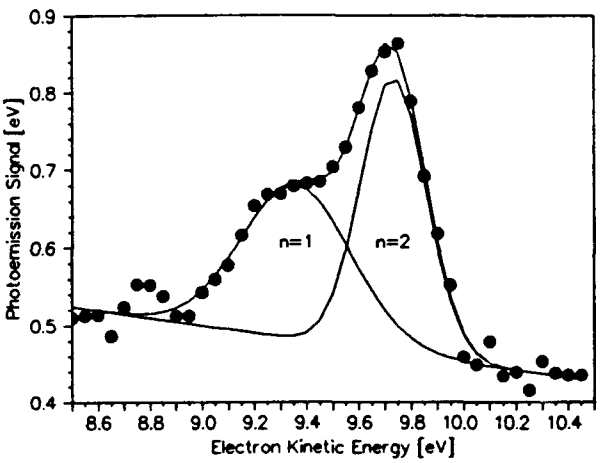

Figure 12 Electron energy distribution curve from Cu(110), excited with hν=4.16 eV photons.

A3. Modelling of Photoelectron Space-Charge Effects during Intense Laser Irradiation

A physical model has been developed to describe the broadening of the energy spectrum of photoemitted electrons in the presence of intense ultraviolet radiation. This model is important for interpreting laser photoemission experiments and for modeling laser photodiodes.

---

[44] P.M. Echenique and J.B. Pendry, *Prog. Surf. Sci. 32, 111 (1990).*

[45] A. Zangwill, *Physics at Surfaces, p. 214 (Cambridge University Press, 1989)*; J.W. Gadzuk, *Surf. Sci. 43, 44 (1974)* and D.M. News, *Phys. Rev. 178, 1123 (1969).*

In this case, electric fields that resulted from the copious electron emission can accelerate some of the electrons up to several times their initial energies and cause most of the emitted electrons to return to the emitting surface.[5] In this model, the Coulomb repulsion among these electrons is considered as the main mechanism which distorts the original electron energy distribution according to the Fokker-Planck equation.[46] The relaxation of the system of electrons depends on both the characteristic time of the experimental measurement and the characteristic collision time of the electrons. Usually, in an ultraviolet photoemission experiment, the time scale of measurement is fixed and can be estimated as the average transit time for an electron reaching the detector after injection from the sample surface. Therefore, the distortion of the electron energy spectrum depends only on the mean electron collision frequency (*i.e.* the reciprocal of the characteristic collision time) which is, in theory, linearly proportional to the electron number density, and so to the ultraviolet laser intensity. Our focus has been onthe modeling of space-charge accumulation due to the continuous electron emission during one single laser pulse and its effect on our experimental results: for instance, in our work on the spectroscopy of image-potential induced states on Cu(100) (see section **A2a**), contributions from space-charge effects in the shifts of the apparent energy position of the image-potential induced states in the electron energy distribution curves were recognized and eliminated. Nevertheless, these effects are of potential interest to the electron spectroscopist and, consequently, we carried out a detailed computerized study of the space-charge induced modifications of electron energy distribution peaks. The space-charge effect of the photoejected electrons were also estimated in the frame

[46] M.N. Rosenbluth, W.M. McDonald and D.L. Judd, *Phys. Rev. 107, 1 (1957)* and W.M. McDonald, M.N. Rosenbluth and W. Chuck, *Phys. Rev. 107, 350 (1957).*

of a simple analytical physical model. Briefly, taking into account the duration of the laser pulse and the geometry of our system, we developed a one-dimensional model which describes well the electrons at the vicinity of the sample surface. As the electrons evolve further away from the surface, we showed that a two-dimensional model is required to describe accurately the dynamics of the space charge. The cross-over between these two limits is determined and corresponds to electrons away from the surface by ~0.1 laser spot size. Finally, we obtained energy shifts, at the detector, for the image-potential induced state electrons, which magnitudes and direction are in excellent agreement with the corresponding experimental results.

B. SPECTROSCOPIC STUDIES OF DIVALENT METAL-ALKYL MOLECULES ON METAL AND SEMICONDUCTOR SURFACES

The conclusion of our ARO research work in understanding and developing the spectroscopy of adsorbed divalent metal alkyls is presented in this section. Significant progress has been made, leading to a working knowledge of the spectroscopic characteristics of adsorbed dimethyl Group IIB-metal molecules, as demonstrated by the fabrication of Schottky diodes to InP and $In_{0.47}Ga_{0.53}As$ by laser photodeposition of Cd.

B1. Introduction

B1a. Background

Some of the earliest demonstrations of both the fundamental chemistry and practical applications of laser chemical processing techniques involved photofragmentation of relatively

simple metal-alkyl molecules.[47,48,49,50,51] For example, laser direct writing of metal lines[47] and direct doping of compound semiconductors were first demonstrated[48] with two related organometallics, *i.e.* dimethyl cadmium (DMCd) and diemethyl zinc (DMZn). Both of these molecules were also used in the first demonstration of additive mask repairs[51] and circuit testing and restructuring.[52] Metal alkyls were attractive sources because they are easily fragmented in the medium ultraviolet range with readily available pulsed and ultraviolet laser sources. The photochemical processing techniques utilizing these molecules involve a complex series of heterogeneous chemical processes. For example, in the photodeposition of metal films, most metal atoms in the deposit result from photolysis of either gas-phase or physisorbed species. On the other hand, the patterning or spatial resolution of the process results, to a large degree, from photolysis of chemically adsorbed molecules.[53,54] Simple metal alkyls form a useful class of model compounds for investigating photochemical interfacial phenomena.

---

[47] T.F. Deutsch, D.J. Ehrlich and R.M. Osgood, Jr., *Appl. Phys. Lett. 35, 175 (1979).*

[48] D.J. Ehrlich, R.M. Osgood, Jr. and T.F. Deutsch, *Appl. Phys. Lett. 36, 916 (1980).*

[49] T.F. Deutsch, D.J. Ehrlich, R.M. Osgood, Jr. and Z.L. Liau, *Appl. Phys. Lett. 36, 847 (1980).*

[50] D.J. Ehrlich, J.Y. Tsao, D.J. Silversmith, J.H. Sedlacek, W.S. Graber and R. Mountain, *IEEE Elect. Dev. Lett. EDL-5, 32 (1984).*

[51] D.J. Ehrlich, T.F. Deutsch, D.J. Silversmith and R.M. Osgood, Jr., *IEEE Elect. Dev. Lett.EDL-1, 101 (1980).*

[52] T. Cacouris, R.R. Krchnavek, H.H. Gilgen R.M. Osgood, Jr., S. Kulik and J. Schoen, *Proceedings of the IEDM (1985).*

[53] D.J. Ehrlich, R.M. Osgood, Jr. and T.F. Deutsch, *J. Vac. Sci. Technol. 20, 738 (1982).*

[54] D.J. Ehrlich, R.M. Osgood, Jr. and T.F. Deutsch, *Appl. Phys. Lett. 38, 1 (1981).*

Metal-containing parent molecules appear in both the divalent and trivalent forms with a wide variety of substituted ligands. This structural and chemical diversity allows the effects of various molecular properties to be studied systematically. Further, the ultraviolet spectra of these molecules occur in the easily accessible near-to-medium ultraviolet region and exhibit characteristic and distinguishing features. The significant vapor pressure of most of these compounds, allows for convenient study of both gas and adsorbed phases at room temperature. Finally, their simple molecular structure allows a clear physical interpretation. These properties, along with the fact that divalent metal-alkyls have been used as a series of metal source molecules for various photon and thermal processing techniques for microelectronics,[55] have led us to a series of experiments on both gas- and surface-phase metal-alkyl photochemistry, in the last decade. Dimethyl cadmium (DMCd) was used in one of the first demonstrations of the photofragmentation anisotropy in gas-phase photodissociation,[56] an experiment which interestingly relied on the observation of Cd-metal deposition on the walls of the glass cell. Subsequently, studies using lasers,[57] synchrotron radiation,[58] and ultraviolet spectroscopies allowed the first two electronic excited states of the dimethyl Group IIb metal alkyls to be

---

[55] See for example, R.M. Osgood, Jr., *Ann. Rev. Phys. Chem. 34, 77 (1983)* and D.J. Ehrlich, R.M. Osgood, Jr. and T.F. Deutsch, *IEEE J. Quantum Electron. 16, 1233 (1980).*

[56] C. Johnah, P. Chandra and R. Bersohn, *J. Chem. Phys. 55, 1903 (1980).*

[57] J.O. Chu, G.W. Flynn, C.J. Chen and R.M. Osgood, Jr., *Chem. Phys. Lett. 119, 206 (1985)* and S.L. Baughcum and S.R. Leone, *Chem. Phys. Lett. 89, 183 (1982).*

[58] C.F. Yu, F. Youngs, K. Tsukiyana, R. Bersohn and J. Preses, *J. Chem. Phys., 85, 1382 (1986).*

determined and analyzed theoretically[59] The spectra of adsorbed molecules have been measured in both their chemi- and physisorbed phases by ultraviolet and infrared techniques.[60,61,62]

Finally, ultra-high vacuum surface analysis techniques have been used to determine the chemical state of these molecules adsorbed on silicon surfaces.[63] For the trimethyl alkyls, extensive measurements have also been reported. However, the overall picture is more complicated because of the greater number of ligands. The gas-phase ultraviolet photodecomposition of these molecules has been discussed and analyzed by Motooka and co-workers.[64] In addition, infrared photoacoustic techniques have been used by Higashi[65] to study the photochemical reaction rates on sapphire substrates. Finally, Greene *et al.*[66] and

---

[59] C.J. Chen and R.M. Osgood, Jr., *J. Chem. Phys. 81, 318 and 327 (1984).*

[60] C.J. Chen and R.M. Osgood, Jr., *Chem. Phys. Lett. 98, 363 (1983).*

[61] E. Sanchez, P.S. Shaw, J.A. O'Neill and R.M. Osgood Jr., *Chem. Phys. Lett., 147, 153 (1988).*

[62] P.S. Shaw, E. Sanchez, Z. Wu and R.M. Osgood, Jr., *Chem. Phys. Lett. 151, 449 (1988).*

[63] C.D. Stinespring and A. Freedman, *Chem. Phys. Lett. 143, 153 (1988).*

[64] T. Motooka, S. Gorbatkin, D. Lubben and J.E. Greene, *J. Appl. Phys. 58, 4397 (1985),* T. Motooka, S. Gorbatkin, D. Lubben, Djula Eres and J.E. Greene, *J. Vac. Sci. Technol. A 4, 3146 (1986)* and D. Eres, T. Motooka, S. Gorbatkin, D. Lubben and J.E. Greene, *J. Vac. Sci. Tech. B 5, 848 (1987).*

[65] G.S. Higashi, L.J. Rothberg and G.C. Fleming, *Chem. Phys. Lett. 115, 167 (1985).*

[66] D. Lubben, T. Motooka, J.E. Greene and J.F. Wendelken, *Phys. Rev. B 39, 5245 (1989).*

White *et al.*[67] have used a variety of surface analysis techniques to study the photo- and thermo-decomposition of trimethyl aluminum (TMAl) on silicon surfaces.

B1b. Spectroscopy of dimethyl Group IIB metal Molecules in the Gas Phase

We would like to start this section by a brief preliminary discussion of the molecular structure and ultraviolet spectra of the isolated (*i.e.* in a gas phase) dimethyl cadmium molecule and, more generally, of the divalent metal-alkyl molecules. To a first approximation, the electronic states of the gas-phase Group IIb metal alkyls can be examined in terms of only the four outer electrons which occupy the bonding sp^3-hybrid orbitals. Such a four-electron picture has been verified by an *ab initio* calculation of the electron structure of the ground state of dimethyl cadmium.[68] Within this approximation, the divalent metal alkyls resemble closely the simplest polyatomic molecules: metal dihydrides with four active electrons (BeH_2, MgH_2, ..., CdH_2). As indicated by Walsh,[69] these four-electron dihydrides should be linear in their ground state and bent in their first excited state. Note in the discussion that follows, we will use, for simplicity, the approximate symmetry of point group $D_{\infty h}$ for linear electronic state and C_{2v} for the bent molecule due to the quasitriatomic nature of the molecule. The two excited states of the dimethyl alkyls give rise to two prominent absorption bands which characterize the divalent metal alkyls. Excitation of the molecule to the first excited state (A^1a), results in the immediate production of a bent "quasitriatomic" molecule. This correlates to an electronic

---

[67] Y. Zhou, M.A. Henderson and J.M. White, *to be published.*

[68] G.M. Bancroft, D.K. Creber and H. Basch, *J. Chem. Phys. 67, 4891 (1977).*

[69] J. Walsh, *J. Chem. Soc. 2260 (1953).*

ground-state monomethyl molecule and a methyl radical. The monomethyl molecule is highly vibrationally excited and undergoes subsequent predissociation into a methyl radical and a Cd atom. Since this first excited state is strongly repulsive; absorption to this state is broad and featureless. The second excited state, $B^1\Pi_u$, is linear and contains a nonbonding, excited π orbital. Consequently, the molecule dissociates immediately into an electronically excited ($^2\Pi_{1/2}$, $^2\Pi_{3/2}$) monomethyl molecule and a methyl radical. The potential surface of this excited state has a saddle point and two troughs,[59] a structured continuum is observed in the absorption spectra, indicating that the lifetime of the excited state is longer than a vibrational period. Ultimately, the electronically excited monomethyl species radiatively decays to the ground state. This state has recently been observed by Yu *et al.*[58] The absorption spectra for these metal alkyls correspond to dipole-allowed transitions and have relatively strong integrated absorption strengths. For DMZn, the transition to the bent excited state is stronger than the linear excited state. For DMCd, the opposite is true. The photodeposition of Cd has been investigated previously and is known to yield high quality, low resistivity Cd films.[70]

We studied the photodissociation dynamics of DMCd as a function of wavelength in the gas phase and for adsorption onto various substrates.[71,72] The ultraviolet absorption spectrum of gas phase DMCd consists of a weak continuum structure starting at ~275 nm and a much stronger peak starting ~232 nm and centered around ~218 nm (~46000 cm^{-1}). The

---

[70] H.H. Gilgen, C.J. Chen, R. Krchnavek and R.M. Osgood, Jr., in *Laser Diagnostics and Photochemical Processing, D. Bauerle ed., pp. 225-233 (Springer-Verlag, New York, 1985).*

[71] C.J. Chen and R.M. Osgood, Jr., *Appl. Phys. A 31, 172 (1983).*

[72] P.S. Shaw, *Ph.D. dissertation (Columbia University, New York, 1989).*

absorption cross-sections associated with 248- and 193-nm radiation (two excimer laser wavelengths which we used in our experiments) lie on opposite shoulders of the two features and are comparable in magnitude. Absorption of a single ultraviolet photon at either wavelength promotes the DMCd molecule to one of two dissociative states which each result in the loss of both methyl ligands. This work has further shown that metal films can be photodeposited from either adsorbed or gas phase molecules, with the relative importance of these two phases being determined by the temperature and conditions at the surface. For instance, at relatively low pressure (*i.e.* well below the DMCd vapor pressure) and room temperature, for which conditions deposition occurs, it is likely that the gas phase photodissociation dominates over any contribution from physisorbed molecules. In addition, while it is clear that a ~1 monolayer phase of partially and completely dissociated DMCd molecules forms on the surface, the X-ray photoemission spectroscopy study presented below, as well as photochemical studies on related systems,[72] shows that this phase is not photochemically altered by irradiation at 248-nm.

B2. Adsorbed Cd on Si and SiO_2

These studies focus primarily on species adsorbed on amorphous SiO_2, which occurs both in the form of a pure bulk substrate or as a thin surface layer on silicon. On this substrate the alkyls appear both in the chemically and physically (liquid-like) adsorbed phases. In either of these phases, the molecules adsorb in their undissociated state, with the binding sites being OH groups for chemisorbed molecules and the chemisorbed alkyl molecules for physisorbed molecules. The attachment of the alkyl molecules via the OH bonds provides a unique opportunity to examine the photochemistry of molecules which are attached to the surface via

an intermediate species rather than adsorbed directly on a bare surface. Our studies indicate that the photophysics changes dramatically from that exhibited in the gas phase, despite the fact that amorphous SiO_2 is itself a passive surface. Further, our studies show that the photophysics, and specifically the reaction yield depend critically on which spectral region of the adsorbed molecule is examined.

B2a. Experimental

In the presence of an overlying gas ambient at room temperature, the adsorbed state of the dimethyl metals at room temperature consists of two distinct phases: weak physisorbed layers and a more strongly adsorbed chemisorbed layer. The first phase is maintained only in the presence of a gas ambient; thus, any surface techniques used to study this phase must be capable of both operating under relatively high pressure conditions and distinguishing the surface-bound molecules from those in the gas above it. The second phase, the chemisorbed layer, maintains its integrity without an ambient gas and can be studied under ultrahigh vacuum conditions. This work is concerned primarily with chemisorbed molecules. The metal-alkyl gases (dimethyl zinc and dimethyl cadmium, electronic grade 99.99%) used in this work were purified by several freeze-pump-thaw cycles at liquid-nitrogen temperature prior to introduction into the sample cell. Gas was admitted into the cell through a bakeable stainless-steel gas-handling system, and the pressure of the gas was monitored with a capacitance manometer. A variety of techniques were used in this work to examine the surface-phase chemistry and spectroscopy of metal alkyls.

Infrared absorption spectroscopy using the technique of total internal reflection was sensitive to submonolayer coverages. The apparatus used for these experiments is described in

detail in Reference 61 and in previous reports. This technique was used to measure the vibrational spectra of methyl-containing species and to detect surface-OH groups. Photochemical changes in the adsorbed molecules were examined upon irradiation with an excimer laser, operating at the wavelengths 193 nm or 248 nm. Low laser fluences were maintained to avoid laser-heating effects (see below). The polished silicon internal-reflection element[73], used in these experiments was chemically degreased using a standard microelectronic device cleaning procedure. Prior to mounting in the vacuum cell, the element was subject to successive treatments with H_2SO_4/H_2O_2 (1:1) and HF (10%) solutions.[74] For experiments on oxidized silicon, the final treatment was with H_2SO_4/H_2O_2, while hydrogen-passivated surfaces were prepared with a final treatment of a dilute HF solution. The latter passivated surface is hydrophobic and has been characterized as unreactive for extended periods of time (up to 1 hour under atmospheric conditions).[75] This chemical stability is due to the presence of hydrogen atoms at each silicon dangling bond site at the surface. The infrared-absorption feature corresponding to the Si-H vibration could be seen for these sample surfaces.[76] For the H_2SO_4/ H_2O_2 treated silicon, a thin oxide layer, approximately 50-Å thick, remains on the surface. A ubiquitous layer of OH groups is present on such oxidized surfaces after exposure to air or water. Such surface OH groups have been studied previously, predominantly on porous

---

[73] N.J. Harrick, *Internal Reflection Spectroscopy (Harrick, Ossining, 1979).*

[74] W. Kern, *Semicond. Int. 94 (April 1984).*

[75] Y.J. Chabal, G.S. Higashi and S.B. Christman, *Phys. Rev. B 28, 4472 (1983).*

[76] V.A. Burrows, Y.J. Chabal, G.S. Higashi, K. Raghavachari and S.B. Christman, *Appl. Phys. Lett. 53, 998 (1988).*

silica.[77] These studies have illustrated that the density of OH groups depends on the evacuation and thermal history of the surface. Typically, heating of oxide surfaces to 200 °C under high vacuum condition for several hours leaves an OH density of $\sim 5 \times 10^{14}$ per cm^2. This value decreases at higher temperatures.

Ultraviolet absorption spectroscopy employing a single-pass technique was used to examine the optical absorption on a single surface of transparent material.[62] The technique used a double-beam spectrometer to detect the ultraviolet absorption of molecules on a bulk SiO_2 sample. The ultraviolet absorption signal due to chemisorbed layers was observed by carefully subtracting a background trace, obtained prior to exposure of metal alkyls, from a signal observed after exposure of the substrate to several Torr of metal-alkyl gas. An ultraviolet absorption of less than 0.1% could be detected and reproducible signals were obtained from 190 nm to 900 nm at coverages estimated to be as low as 0.1 monolayer. The sample cell could be baked to a temperature of 600 °C at a residual pressure of 10^{-8} Torr.

Thermal- and photo-desorption mass spectroscopy were also used to investigate surfaces. In these cases, a bakeable stainless-steel sample cell was equipped with ultraviolet-transmitting windows and a quadrupole mass spectrometer for detecting the parent metal alkyl and any of its radicals or molecular fragments which were created after laser irradiation or resistive heating of the surface. A sample surface is dosed in a substrate preparation chamber and subsequently transferred to the analysis main chamber, in order to prevent contamination of this chamber with the metal-alkyl gas. The sample surface, which consisted of SiO_2-covered silicon, was prepared as described above. Desorption experiments were performed under continuous-pumping

---

[77] L.H. Little, *Infrared Spectra of Adsorbed Species (Academic Press, New York, 1966).*

conditions, with the evacuation rate being rapid compared to the repetition rate of the excimer laser. Nonetheless, any species desorbed from the surface during laser or thermal excitation suffered many collisions with the wall prior to detection in the mass spectrometer. For the thermal desorption experiments, the sample surface temperature was raised with a resistive heater. Typically, the heating rate was 1.1 K/s. The sample surface temperature was monitored by a thermocouple placed directly in contact with the sample surface. In the laser desorption experiments, the beam from an excimer laser ($\lambda = 193$ nm or 248 nm) entered the main chamber through a ultraviolet-quartz window of 80° off the surface normal of the sample. The typical excimer laser fluence was less than 1 mJ/cm^2 per pulse with a 10-Hz repetition rate. Neither the peak power per pulse nor the average power was sufficient to heat the sample under these conditions.[78]

B2b. Spectroscopy of Adsorbed Layers

The infrared and ultraviolet spectroscopic studies of the chemisorbed layers can each be used to understand different aspects of the photophysics of the physisorbed molecular layer. In particular, the infrared spectra are most useful for probing the methyl ligands of the adsorbed molecules. The ultraviolet measurements directly address the question of changes in the electronic states after the molecule binds to the surface.

B2bi. Infrared Spectroscopy

Fourier-transformed infrared spectra of adsorbed DMCd were recorded in the region

---

[78] V. Liberman, *private communication.*

from 2 to 6 μm, where absorption bands corresponding to CH stretching vibrations of the methyl ligands occur for the gas-phase molecule. Figure 13 shows the infrared spectra of the chemisorbed molecules in the region of the CH stretch frequency. The chemisorption traces were observed upon evacuation of a previously gas-filled sample cell for several hours to a pressure of $\sim 1 \times 10^{-8}$ Torr. As will be explained below, the magnitude of these absorption features is sensitive to the chemical and thermal history of the sample during preparation. The absorption frequencies of the bands in Figure 13 (2975, 2928 and 2863 cm^{-1}) are nearly coincident with those of the gas-phase molecule,[79] and they remain constant with increasing DMCd pressure. Experiments were also performed to observe the 3-μm stretching vibrations of OH on the SiO_2 surface, since they will be shown below to be important for the process of chemisorption of the alkyl species. We were able to observe the O-H stretching vibrations of a silicon surface covered with native oxide. The oxide surface was prepared as described above and evacuated at 100 °C for 24 hours. The spectrum was obtained by normalizing the total internal reflection signal of this oxide surface by the signal from a separate measurement with a hydrogen-passivated surface (*i.e.* no surface OH groups). A broad absorption feature around 3500 cm^{-1} corresponds to hydrogen-bonded O-H stretching vibrations as shown in Figure 14. However, no discernible isolated O-H groups can be observed at 3750 cm^{-1}, probably due to the low-bake-out temperature.

[79] I.S. Butler and M.L. Newbury, *Spectrochim. Acta 33 A, 669 (1977).*

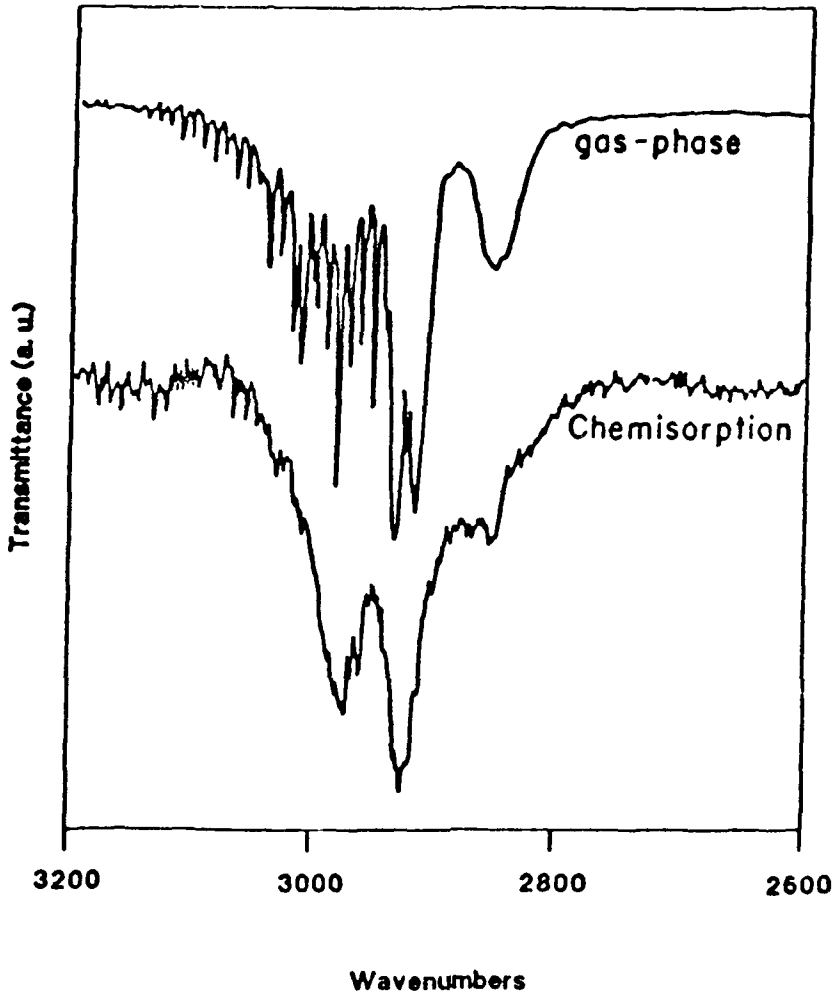

Figure 13 Fourier-transformed spectra of the chemisorbed and gas-phase DMCd molecules, with a background pressure of 1×10^{-7} Torr. The intensity in each trace in normalized to the peak intensity of the corresponding trace.

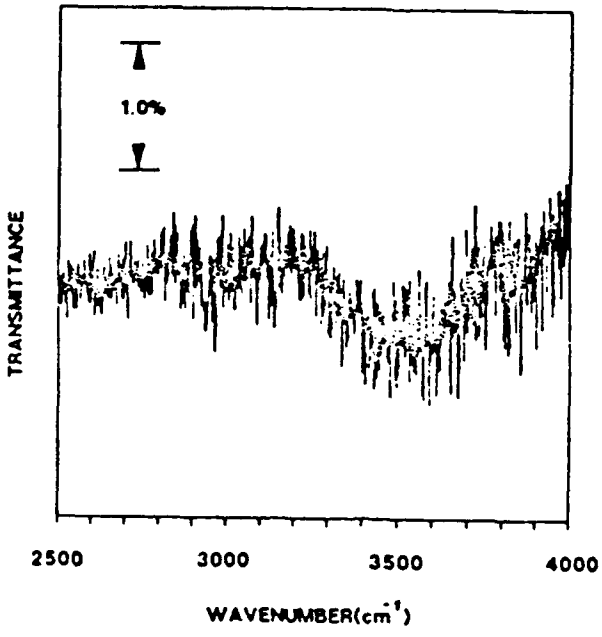

Figure 14 Infrared absorption spectrum due to hydrogen-bonded OH groups on a SiO_2 surface.

B2bii. Ultraviolet Spectroscopy

The ultraviolet measurements of chemisorbed dimethyl zinc and molecules are shown in Figure 15. A comparison of the ultraviolet spectra of the gas-phase and chemisorbed molecules, both in the infrared and ultraviolet regions of the spectrum, illustrate that beside some broadening and slight frequency shifts, no major change spectral occurred. This behavior suggests that the metal-alkyl molecules are not dramatically perturbed on surfaces and the gas-phase spectra can serve as a very useful guide for the transitions which occur on surfaces.

B2c. Nature of the Adsorbed Molecular Species

The metal-carbon bond in metal alkyls is not strong, *i.e.* the first CH_3 ligand in DMCd is bound by only 48.8 kcal/mole. In addition, metal alkyls are known to react strongly with water, O_2, and other molecules, fragments of which may be adsorbed on surfaces such as SiO_2. As a result, it is important to determine the specific molecular species which adsorbs on the substrate surfaces and what is the adsorption site for this species. Note that the relatively strong bond between the molecules and the surface, as shown by the integrity of the adsorbed layer under many hours of ultrahigh vacuum conditions is indicative of strong surface bonding.

B2ci. Nature of the Chemisorbed Molecules

In order to determine the nature of the chemisorbed species, we performed temperature programmed desorption on SiO_2 surfaces exposed to either DMCd or DMZn. Shown in Figure

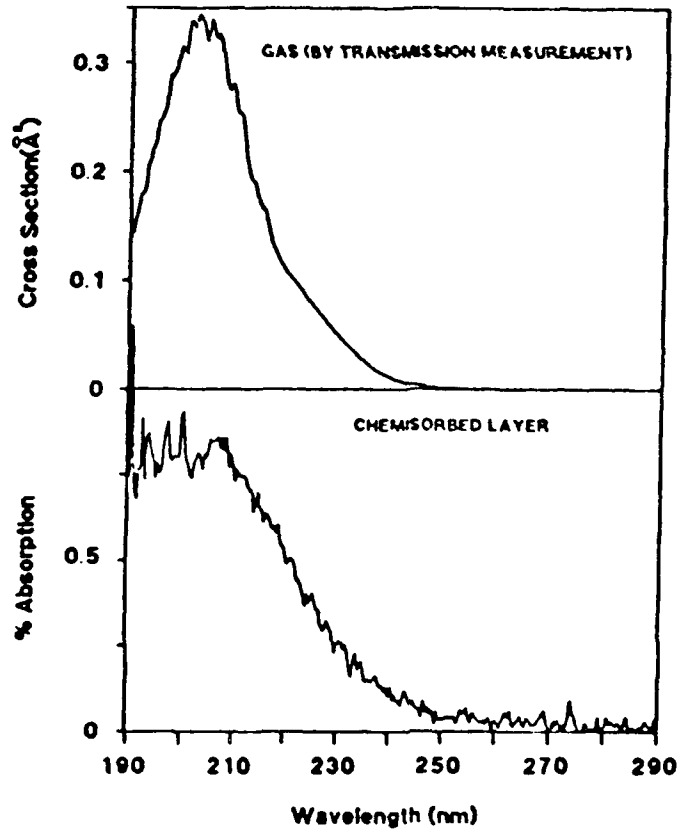

Figure 15 Ultraviolet spectra of (a) gas-phase DMZn (b) chemisorbed DMZn on a single crystal quartz surface heated to 120 °C for 24 hours prior to the formation of a chemisorbed layer.

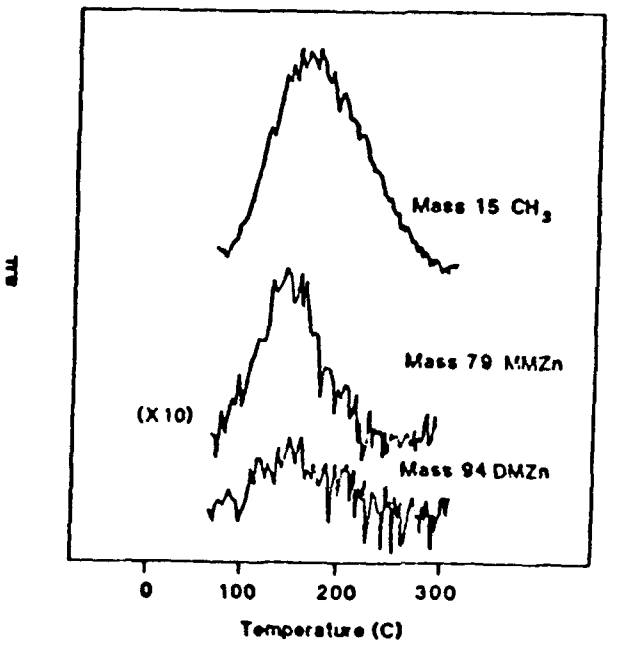

Figure 16 Temperature-programmed desorption signal of chemisorbed DMZn on SiO_2 with 1.1 K/s heating rate.

16 is the mass-spectrometer signal of masses 15, 79 and 94 observed from desorption of a surface previously exposed to dimethyl zinc at a heating rate of 1.1 K/s. The cracking pattern is measured to be the same as the gas-phase DMZn pattern, thus indicating that the nascent desorbed species was only DMZn. Note that heating to higher temperatures than those shown in the figure did not result in desorption of any additional species. Furthermore, ultraviolet absorption spectroscopy was used to examine chemisorbed species on a SiO_2 surface prior to and after a thermal treatment similar to that used in the temperature-programmed desorption experiments. The results showed the disappearance of absorption features after heating to 100 °C for 5 minutes (see Figure 17). This behavior is consistent with the desorption of all species on substrate surface. In addition, the ultraviolet experiments showed that the number of adsorbed molecules present after thermal desorption and subsequent exposure to a second dosage was nearly identical to that after the initial dosage. We will return to this point below. A similar set of experimental results were obtained using dimethyl cadmium molecules. These results indicate that the surface-bound species is the undissociated metal alkyl. These findings are in accord with the somewhat more tentative conclusions reached by Stinespring and Freedman[63] using the chemical shifts of cadmium on SiO_2 with X-ray photoemission spectroscopy. The results are also in accord with the fact that both the infrared and ultraviolet spectra of the chemisorbed molecules resemble the free-molecule absorption bands with minimal perturbations due to the effects of surface bonding. The chemical behavior of the molecules on the surface is also in accord with their identification as undissociated dimethyl species. In particular, the change of both the ultraviolet and infrared spectra, which is observed when water vapor was introduced upon chemisorbed layer, supports the existence of a carbon-metal bond

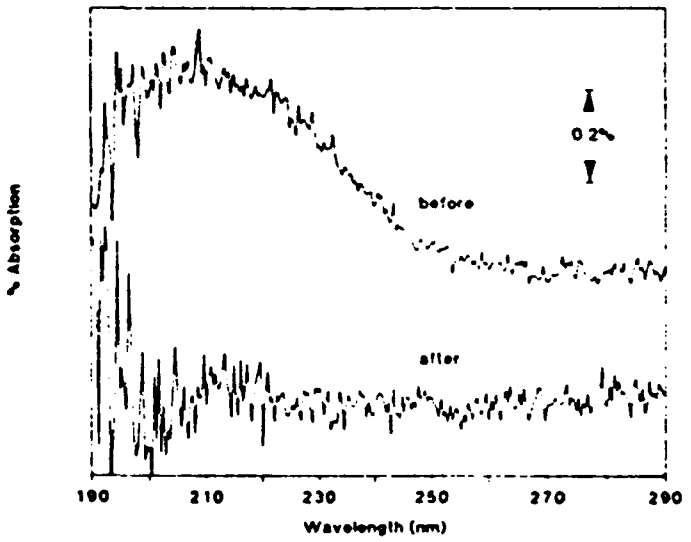

Figure 17 (a) Spectrum of chemisorbed DMCd molecules on quartz, (b) the same system after being heated to 100 °C.

which is extremely reactive to water.

B2cii. Binding Sites of the Adsorbed Molecules

As indicated in the introduction, the dimethyl-metal absorption systems described here present an interesting opportunity to study the photochemistry of target molecules which are bound to the surface via a second adsorbed entity. The purpose of this section is to provide the experimental evidence for identifying the chemisorption binding site as surface-adsorbed OH molecules and for showing that the chemisorbed dimethyl metal molecules serve as binding sites for the physisorbed molecules. Both ultraviolet and infrared spectroscopies were used in this determination. The first set of experiments used total internal reflection spectroscopy to measure the number of molecules adsorbing on the surface after various methods of surface preparation. In these experiments, the silicon optical element was first prepared so that it contained a significant amount of surface oxide by means of the H_2O_2: H_2SO_4 treatment mentioned above. A second surface was prepared by an HF treatment to achieve hydrogen passivation. Typical absorption spectra for physisorbed and chemisorbed dimethyl cadmium present on both oxidized and passivated silicon surfaces are presented in Figure 18. The physisorption spectra were again obtained using 30 Torr of ambient DMCd gas. The results show clearly that the number of chemisorbed molecules appears to correlate with the amount of SiO_2 present on the surface. Further experiments on surfaces which had a thin covering of native-oxide and those where the oxide was thicker again showed that the extent of surface oxidation determined the amount of adsorbed species. Note that the method of oxide formation used to obtain the data in Figure 18 does not clearly distinguish an oxide surface adsorption site from a silanol species which is

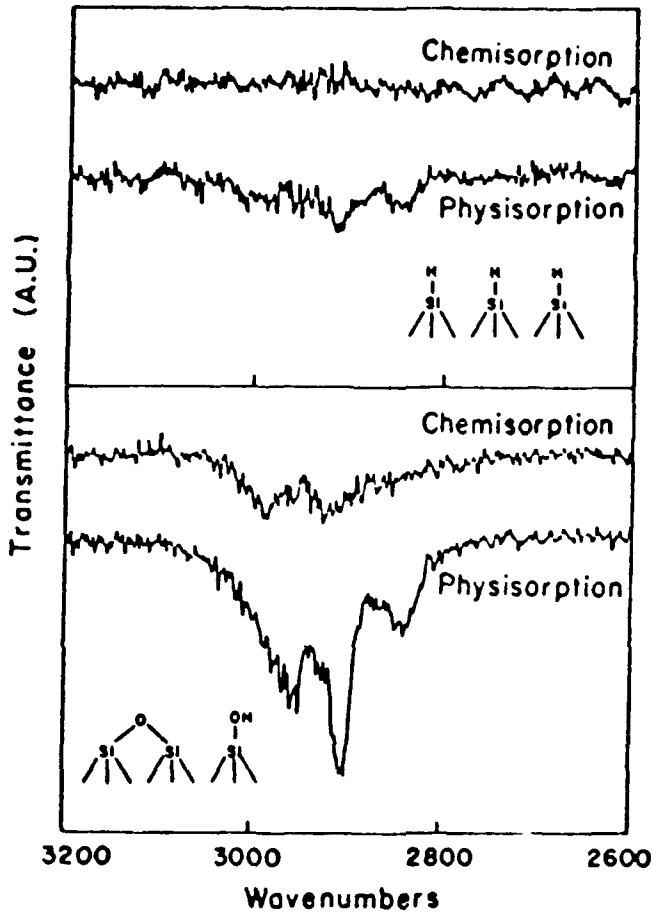

Figure 18 Infrared absorption spectra of DMCd on both oxidized silicon and silicon passivated by a monolayer of atomic hydrogen.

present on all oxides exposed to water vapor. In order to remove this ambiguity, we performed a second series of experiments with ultraviolet spectroscopy. Ultraviolet spectroscopic studies performed on fused-silica substrates showed that the amount of absorption is also controlled by the extent of preheating of the silica surface.[62] In these experiments an SiO_2 surface was baked at varying temperatures for 24 hours. The cooled surface was then exposed to 10 Torr of either DMCd or DMZn for 1.5 minutes and an ultraviolet absorption spectra was recorded after evacuation of the chamber. As shown in Figure 19, preheating temperatures of ~500 °C are sufficient to reduce by a factor of four of the amount of surface adsorption on the silica. Shown in the insert of Figure 19 is the dependence of the ultraviolet absorption intensity at 210 nm and the prebaking temperature. It correlates well with the known thermal removal of surface-hydroxyl radicals with temperature.[77] These results suggest that the primary absorption site is the surface OH groups and not the simple silicon oxide sites. In connection with this ultaviolet experiment, after the chemisorbed layer was formed and its ultraviolet spectra observed, the surface was baked again to 150 °C and the chemisorbed layer was then allowed to form again after cooling the surface to room temperature. The final ultraviolet absorption signal for the second layer was within 10% of the first indicating that the surface binding sites are unchanged by thermal desorption of the chemisorbed species. The temperature programmed desorption measurement described earlier was used to determine the strength of the adsorbing bond for the dimethyl metal molecules. The sample surface was dosed with 10 Torr of gas to allow chemisorption to occur. After pump down, the sample was transferred to the main chamber and isolated with respect to the preparation chamber. The background pressure was ~10^{-9} Torr, and no contamination was observed from the heater surfaces. The desorption curve for both DMZn

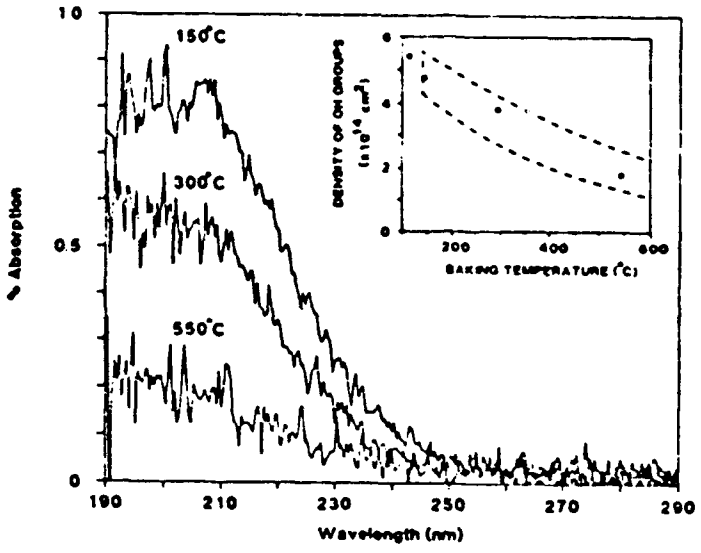

Figure 19 Ultraviolet absorption spectra of chemisorbed DMCd molecules on a quartz surface which has been prepared by baking and evacuating the surface at (a) 120 °C, (b) 300 °C and (c) 550 °C for 24 hours. The insert describes the surface concentration of OH groups as a function of the temperature of the thermal treatment. The hatched area is the range of OH group concentration on silica samples as measured by previous workers[77]. The points are obtained by the present absorption measurement as described in the text. Since only relative values of OH group density can be estimated in our absorption measurement, we have assumed, in plotting the points, that the OH group concentration at 120 °C is equal to the value given in Reference 77.

and DMCd was relatively broad, possibly due to the amorphous nature of surface oxide. The bonding energy, as determined by the peak desorption temperature is 1.1 eV. Further, the relative strength of desorption signals after a thermal desorption run were found to be within 10% of the strength of the initial run, a result similar to that found with the ultraviolet spectroscopic experiments described above. These observations raise a number of questions regarding the nature of the molecular binding to the surface site. More reactive species, such as trimethyl aluminum are known to react strongly with silanol groups through displacement of a methyl ligand and subsequent formation of oxides and methane for TMAl. Both DMCd and DMZn are less reactive than TMAl and might instead be expected to form a complex with the OH groups. In addition, complexes which involve electron-donating groups such as bridging oxygen (e.g. tetrahydrofuran) have been previously isolated.[80] These considerations led us to attempt to determine directly whether adsorption results in the reaction of the alkyl molecules with the surface OH groups. To do this, we used total internal reflection spectroscopy to study the effect of dimethyl metal exposure directly on the OH group, and found that upon introducing the chemisorbed dimethyl cadmium molecule, no change, to within 10%, could be observed in these OH absorption features which are dominantly hydrogen-bonded OH groups. These results seem to indicate that the hydrogen-bonded OH groups remain intact after adsorption of the chemisorbed layer. Similar results were also reported by Yates *et al.*[81] and Higashi *et al.*[65] for adsorption of TMAl on both SiO_2 and sapphire surfaces. In particular, Yates reported, that

---

[80] K. Nutzel in *Houben-Weyl, Methoden der Organischen Chemie, 4th Ed., E. Muller ed., XIII/2a, p. 859 (Thieme, Stuttgart, 1973).*

[81] D.J.C. Yates, G.W. Dembinski, W.R. Kroll and J.J. Elliott, *J. Phys. Chem. 73, 911 (1969).*

only isolated-OH groups were dramatically reduced after adsorption of TMAl leaving the hydrogen-bonded OH groups unchanged for the chemisorption of metal alkyls on porous silicon oxide. Finally, from Figure 18 one can also obtain information on the binding sites of the first layer of the physisorbed molecules. In particular, it is clear that the surface density of physisorbed molecules depends critically on the number of molecules which have already been bound to the surface via the chemisorption process. This result is reasonable since the presence of physically adsorbed multilayers at this temperature indicates that the inter-alkyl-molecular forces are relatively strong and, thus, these molecules would form satisfactory absorption sites for the first physisorbed layer.

B2d. Photochemistry of the Adsorbed Molecules

B2di. Experimental Results

Experiments were performed to examine the photochemical behavior of the chemically adsorbed layer, formed on Si/SiO_2 surfaces, upon ultraviolet-laser irradiation at 193 and 248 nm. Due to the small perturbation of chemisorbed molecules by the surface and the relatively large gas-phase absorption cross sections at these wavelengths, we anticipate that any surface photochemical processes are induced through direct absorption of photons by the adsorbate. In the first of these studies, ~60% of one side of a DMCd-dosed internal-reflection element (30% of the total surface area) was illuminated with pulses from an excimer laser. Figure 20 illustrates that upon irradiation with 3.8 mJ/cm^2 at 2-Hz repetition rate of 193-nm wavelength light, the integrated intensities of the observed infrared ν_5-absorption feature decrease to 70% of their original value in ~1.5 min. On the other hand, illumination of the silicon element at

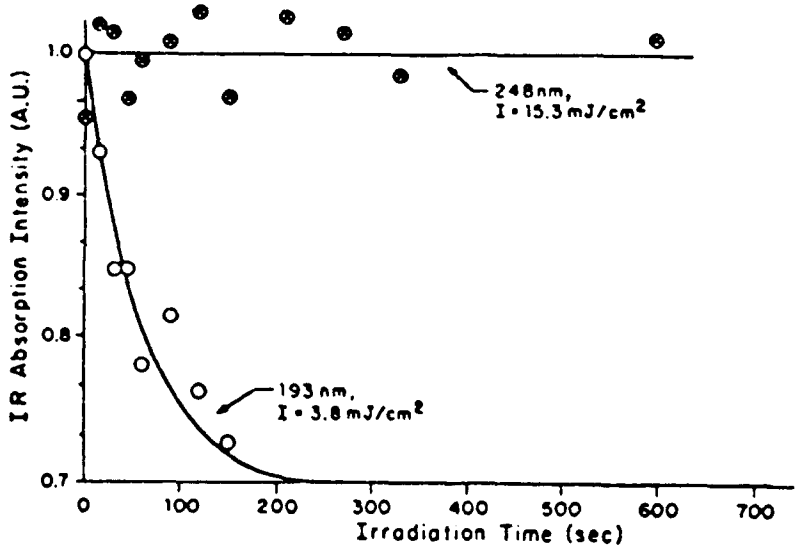

Figure 20 Intensities of the infrared-absorption features of DMCd chemisorbed on oxidized silicon versus time, upon irradiating the sample at both 193 nm and 248 nm.

248 nm, with even higher intensities and for more extended periods of time, cause no observable change in the chemisorption spectrum. The decrease in the chemisorption absorption signal observed at 193 nm corresponds to the photoinduced removal of a CH-containing species from the surface. Thermal-desorption effects are expected to be negligible since the maximum surface-temperature rise during the laser pulse is less than 10 °C at the laser fluences used in these studies.[78] Our temperature-programmed desorption studies indicate that this degree of temperature rise has a negligible effect on the number of adsorbed molecules on the surface. Similar experiments were also performed by measuring the change in the ultraviolet absorption spectrum of chemisorbed DMZn molecules due to excimer-laser radiation. Again, an insensitivity of the molecule to the 248-nm laser wavelength was observed as in the infrared experiment. Upon irradiation with 1 mJ/cm^2 at 193 nm, the ultraviolet-absorption spectrum characteristic of the metal alkyls was observed to broaden gradually and to shift to longer wavelengths (see Figure 21). After 6000 pulses at 10 Hz, the spectra exhibited a broad background absorption which decreased monotonically with wavelength. This spectrum, which is stable to further irradiation, is consistent with the release of methyl groups from the adsorbed layer and the formation of a metal film on the surface. An important aspect concerning the surface photochemical behavior of dimethyl cadmium deals with the nature of the species, which is actually removed by the incident laser. The question of whether the observed decrease in the infrared CH-absorption intensity is due to photolysis of the chemisorbed species or whether it is caused by desorption of the entire chemisorbed molecule must be considered. To distinguish between these two possibilities, experiments were performed using laser desorption spectroscopy. In these experiments, a mass spectrometer was used to observe desorbed metal-alkyl fragments

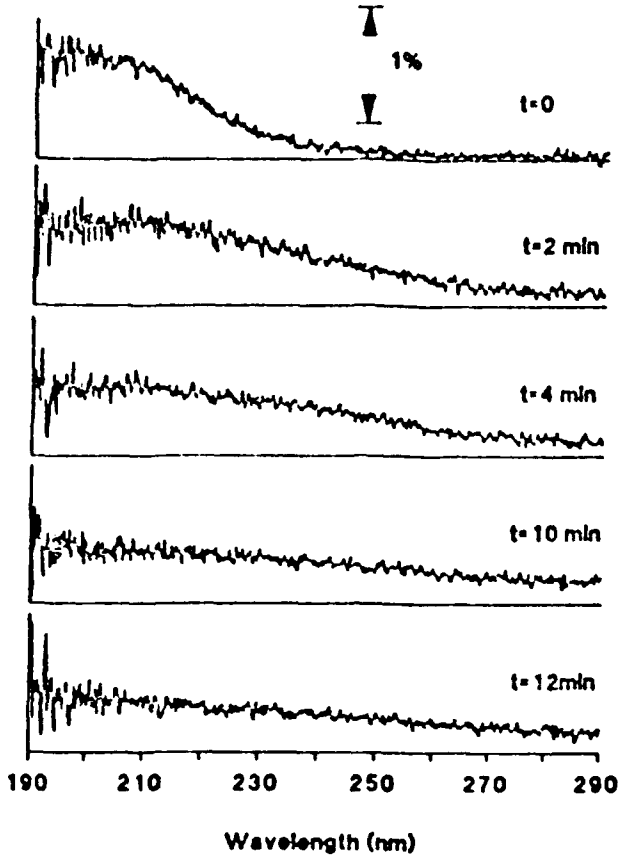

Figure 21 Ultraviolet spectrum of chemisorbed DMZn molecules on a quartz surface, after the layer had been exposed to 0, 2, 4, 10 and 12 minutes of 193-nm laser radiation. The laser pulse repetition rate was 10 Hz.

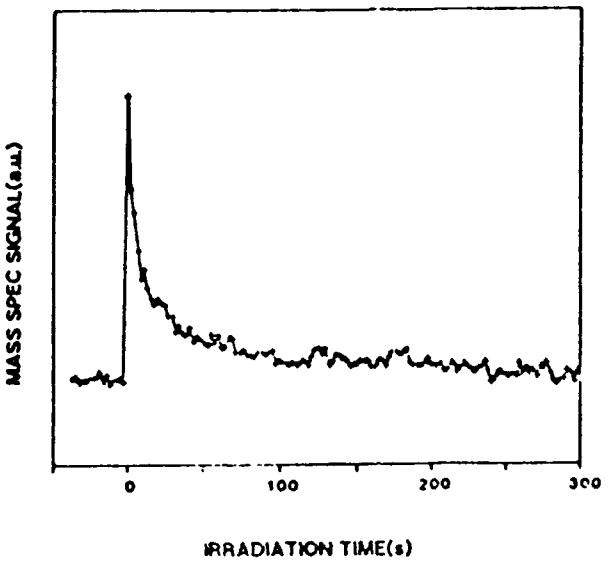

Figure 22 Mass spectrometer signal of laser-induced desorbed CH_3 versus 193-nm irradiation time.

by the laser irradiation. At 193 nm, with a laser fluence of 1 mJ/cm^2 per pulse and 10-Hz repetition rate, only methyl radicalswere observed. Neither dimethyl or monomethyl species were found within the sensitivity of the mass spectrometer. As shown in Figure 22, rather than displaying a single exponential decay, the DMZn desorption signal exhibits an initial fast decay followed by a slower decrease. Again, at 248 nm, no desorption was observed within the sensitivity of our mass spectrometer. The photodesorption results presented in Figure 22 indicate that 90% of desorbed species appear in the slow time decay of the methyl desorption. We believe that the fast decay originates from a small percentage of molecules which are adsorbed on different adsorption sites, although the exact origin of this decay remains unconfirmed. Note that in the two experiments using ultraviolet and infrared spectroscopies to observe changes of adlayers during ultraviolet irradiation by monitoring species left on surfaces (Figure 20), the lower time resolution and smaller signal-to-noise ratio did not allow this fast initial desorbing behavior to be seen. Further laser desorption experiments were performed to determine any effect of photogenerated-carrier chemistry on the adsorbates by changing the thickness of the oxide layer on which adsorption occurs. Several experiments[82] have indicated that such carriers can be responsible for surface photochemistry on semiconductor substrates. In this case, we varied the oxide thickness up to a thickness at which no photocarrier current, *e.g.* via tunnelling, would be expected. However, no discernible difference in the desorption signal was observed to within 10% for oxide thickness ranging from ~20Å to 2000Å. We conclude that desorption due to photogenerated carriers from silicon is not an important mechanism in our experiments. Our final experiment deals with the growth of metal layers by

---

[82] See, for example, W. Ho, *Comments Cond. Mat. Phys. 13, 305 (1988).*

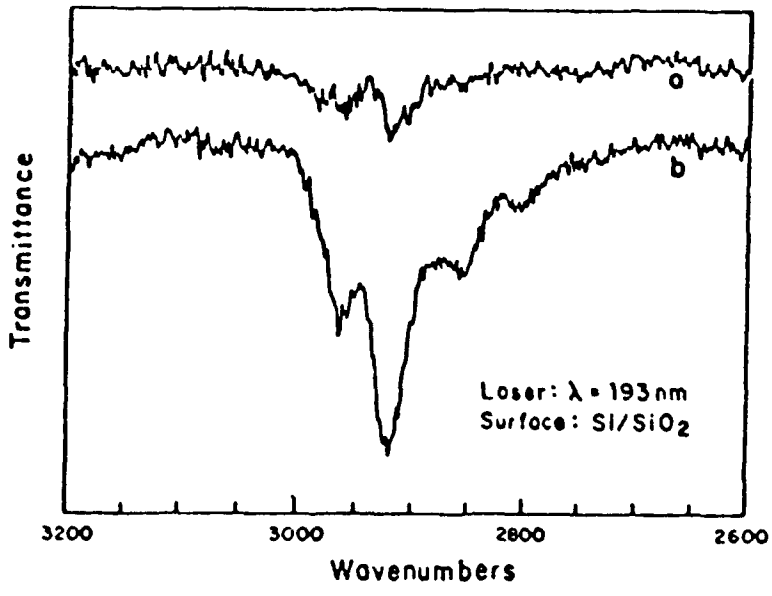

Figure 23 Infrared spectrum of CH stretching region on the SiO_2 surface (a) before and (b) after irradiation at 193 nm inthe presence of 0.2 Torr of DMCd. Note the appearance of a new feature at 2800 cm^{-1}.

irradiating the surface in the presence of ambient gas while monitoring the surface infrared spectrum. The infrared-absorption features resulting from ultraviolet irradiation of Si/SiO_2 surface at 193 nm are shown in Figure 23. The ultraviolet-enhanced absorption due to CH-stretching vibration indicates the incorporation of methyl groups in the surface metal layers. Note that a new band appeared at 2800 cm^{-1} which was not present in the spectrum of either the chemically or physically adsorbed precursor molecule.

B2dii. Surface-Bound Species After Irradiation

Our products seen in our laser-desorption spectroscopy experiments suggest that during laser irradiation, a new overlayer structure is gradually formed on the substrate surface due to the release of CH_3 ligands. A similar behavior has been reported for the photodissociation of surface-adsorbed $Mo(CO)_6$, $W(CO)_6$ and $Fe(CO)_6$ under ultra-high-vacuum conditions; in these cases, a photoexcited metal-to-ligand charge-transfer transition leads to sequential removal of ligands.[83,84] Also, in the case of $Mo(CO)_6$, a new mode ~1500 cm^{-1} appears in the electron energy loss spectroscopy spectrum during the irradiated of 257-nm laser.[83] This mode is attributed to the formation of new overlayer structures through the gradual photodissociation of the adlayer. Our ultraviolet and infrared experiments also support this explanation. First, in the ultraviolet spectral studies of the excimer-laser dissociation process, we observed several

---

[83] C.E. Bartosch, N.S. Gluck, W. Ho and Z. Ying, *Phys. Rev. Lett. 57, 1425 (1986)* and N.S. Gluck, Z. Ying, C.E. Bartosch and W. Ho, *J. Chem. Phys. 86, 4957 (1987).*

[84] J.S. Foord and R.B. Jackman, *J. Opt. Soc. Am. B 3, 806 (1986)* and *Surf. Sci. 171, 197 (1986)*; J.R. Creighton, *J. Appl. Phys. 59, 410 (1986)* and J.R. Swanson, C.M. Friend and Y.J. Chabal, *J. Chem. Phys. 87, 5028 (1987).*

stages as the spectrum of the chemisorbed film shifts to that of the final smooth and structureless, stable spectrum. The intermediate ultraviolet spectra are relatively broad and peak at longer wavelengths than the gas or original chemisorbed spectrum, suggesting a new surface-layer composition. Second, the above mentioned experiment of measuring the infrared spectrum of surface metal layers grown by irradiating the surface in the presence of ambient gas also indicates the interaction of metal and CH_3 ligands left on the substrate surface. In particular, the new feature observed at 2800 cm^{-1} occurs at a frequency which is somewhat lower than that typically expected for a C-H stretching vibration (2840-3100 cm^{-1}), and it reflects a photochemical change in the nature of the species present on the surface after irradiation. Ceyer and also White and their collaborators have previously used high-resolution electron energy-loss spectroscopy to characterize the vibrational spectroscopy of methyl radicals adsorbed on Ni and Pt surfaces.[85,86] In their work, vibrational features were observed in the frequency range between 2690 and 2800 cm^{-1}. These bands were attributed to "soft" CH-stretching vibrations, which result from a hydrogen-bonding-like interaction of the CH_3 group with the metal surface, as would occur for a methyl group which is tilted toward the surface. The additional absorption feature at 2800 cm^{-1} observed in the present experiments is consistent with the presence of such adsorbed CH_3 groups on the surface. Finally, we note that despite the gradual formation of a new metal-rich overlayer structure, our measurements of the photodesorption rate and products are apparently unaffected by its formation. This point can be seen from the exponentiality of the decay of the infrared absorption feature, as well as the constancy of the desorption product.

---

[85] M.B. Lee, Q.Y. Yang, S.L. Tang and S.T. Ceyer, *J. Chem. Phys. 85, 1693 (1986).*

[86] M.A. Henderson, G.E. Mitchell and J.M. White, *Surf. Sci. 184, 1325 (1987).*

The fact that our measurements are heavily weighted toward the initial states of surface photodecomposition because of our finite signal to noise ratio may prevent the change in the overlayer from affecting our measurements.

B2diii. Discussion of the Photophysics

Quantitative values of the ultraviolet cross-sections and reaction yields can be obtained from our experiments. From the experimental results of both infrared and ultraviolet spectra for 193-nm laser irradiation, an estimate of the absorption cross section, σ_{ab}, and the photodissociation cross section, σ_{diss}, for photoremoval of methyl-containing species from the surface can be obtained. The photodissociation yield Y can then be determined by using:

$$Y = \frac{\sigma_{diss}}{\sigma_{ab}} \tag{1}$$

Note that although the experiments in the previous subsection (*e.g.* Figure 21) show that the ultraviolet absorption cross-sections are functions of the decomposed fraction during irradiation, most of our data are obtained with sufficient parent molecules remaining on the surface that the cross-sections can be considered constant during the measurements. All the calculations below are, therefore, valid to a good approximation for the fresh chemisorbed layers.

1. σ_{ab} (Total Ultraviolet Absorption Cross Section)

The ultraviolet transmission spectra mentioned earlier showed a 1% absorption intensity at 193 nm for both chemisorbed DMCd and DMZn molecules(see Figure 15 for DMZn). To estimate the absorption cross section from this absorption intensity requires an *a priori* knowledge of the surface density of metal alkyl species. In our case, it is reasonable to assume

the same surface density for both OH groups and metal alkyl species since surface-OH groups are primarily responsible for metal alkyl chemisorption. For a 120 °C-treated SiO_2 surface, the surface-OH group density can be found from the insert of Figure 19 to be 5×10^{14} cm^{-2} (see Reference 77). Based on this assumption and the fact that the optical absorption coefficient is equal to the product of the surface density and the optical cross section, the absorption cross section at 193 nm for both species is 0.2 $Å^2$. Note that this number is very close to the values of that of the gas-phase molecules(0.2 $Å^2$ for DMZn and 0.1 $Å^2$ for DMCd).

2. σ_{diss} (Photoremoval Cross Section)

By neglecting the change in σ_{diss} with the decomposed fraction of metal alkyl species on the surface, as mentioned above, the temporal change in the number density of the chemisorbed molecular layer due to photoinduced processes on the surface can be expressed as:

$$\frac{dN(t)}{dt} = -\sigma_{diss} N(t) n \tag{2}$$

where N(t) is the number density of chemisorbed molecules at a given time, and n is the flux of ultraviolet-laser photons incident on the sample. Solving this equation yields:

$$N(t) = N_o e^{-\sigma_{diss} n t} \tag{3}$$

where N_o is the number of chemisorbed molecules initially adsorbed on the surface. The cross section can be determined by measuring the characteristic time it takes for both the infrared and ultraviolet absorption signal at a given wavelength to decrease to 1/e of its original value. For example, using the data in Figure 21, a characteristic time of ~40s of laser irradiation is measured, which yields a cross section of 4×10^{-2} $Å^2$ for photoremoval of the chemisorbed

DMCd molecules from the surface. For DMZn, a cross section of 1×10^{-2} Å^2, (~100 seconds for 1/e time), was obtained. In the latter case, we used the change in the ultraviolet absorption spectrum with time for the chemisorbed DMZn molecules. Note that in contrast to the case of the infrared spectrum where coverage-dependent spectral shifts are insignificant, there are more pronounced shifts in the ultraviolet spectra during extended irradiation. However, measurement of σ_{diss} can still be estimated by fitting the absorption decrease, at one wavelength, in the ultraviolet with a simple exponential decay curve and by taking in account the rising broad base line due to the metal atom production.

3. Y (Photoremoval Yield)

The photodissociation yield at 193 nm is easily calculated from σ_{diss} and σ_{ab} to give a yield of 0.2 and 0.05 for chemisorbed DMCd and DMZn, respectively. The fact that the yield for photoexcitation in our surface experiments is much less than unity, both at 248 nm and 193 nm, suggests that an efficient quenching mechanism is operable on the surface which greatly reduces the photodissociation yield from its value of one in the gas phase. Fast adsorbate quenching rate has been generally believed to be more significant for molecules on metal and semiconductor surfaces than on insulators. In the present case, the presence of the surface-OH species may enhance energy transfer to the substrate. The influence of substrate quenching can also be seen in the difference of the yields for excitation at 248 nm and 193 nm. In particular, at 248 nm, the photochemical yield for the chemisorbed species is at least two orders of magnitude smaller than at 193 nm. A possible explanation for this effect appears to lie in the nature of the two different transition states that dominate the gas-phase spectrum at 193 nm and 248 nm. In particular, if energy dissipation into the substrate has a different rate for molecules

in one or the other electronically excited states then the yield at the two wavelengths will be different. For the case of excitation of the gas-phase molecule at 248 nm, predominantly to a bent excited state, dissociation has been shown to be partially due to vibrational predissociation. In particular, the dissociation energy of one methyl group from DMCd is 48.8 kcal/mole and the photon energy at 248 nm is 115.1 kcal/mole. The considerable excess energy of 66.3 kcal/mole (115.1-48.8=66.3) is partitioned among the vibrational and rotational motion of the CH_3 and CH_3Cd fragments and relative translational energy of the ground-state monomethyl cadmium and a methyl radical. The vibrationally excited monomethyl radical then dissociates since its internal energy is greater than the cadmium-methyl bond of ~16 kcal/mole. Recently, Jackson[87] has shown that, in the gas phase, this monomethyl complex is sufficiently long lived that it may be stabilized by inert gas collisions, thus preventing dissociation into Cd and CH_3. If the $Cd(CH_3)_2$ electronic structure on the surface is relatively unperturbed from the gas phase as our ultraviolet data would indicate, a similar process would be expected to quench the excitation of the chemisorbed molecule. Thus, a near vanishing yield at 248 nm is not surprising. At 193 nm, no such detailed gas-phase kinetic data exists; however, it is known that the dissociation physics is considerably different. In particular, the gas-phase dissociation again leads to CH_3 and $CdCH_3$ radicals but the $CdCH_3$ radical is, in this case, electronically excited.[58,59] Since the electronic energy of this radical is considerably lower than the OH electronic states as well as the SiO_2 band gap, there is no direct energy transfer route out of the $CdCH_3$ if placed on SiO_2 surfaces. The radiation to the ground state can still be present leading to dissociation of the monomethyl species. Finally, note that it is possible to view the difference

---

[87] W. Jackson, *unpublished results*.

in photodecomposition at 193 nm and 248 nm from a simpler perspective, namely according to the excess energy above the decomposition energy, placed in the molecule by absorption. In the case of 193 nm, 148 kcal above the dissociation threshold are absorbed into the molecule, at 248 nm only 115 kcal are in excess, if only one CH_3 ligand is removed per absorption event. Clearly, in the latter case relaxation processes such as multiphoton decay will more rapidly stabilize the molecule prior to decomposition. Note that if two CH_3 ligands are removed with each absorption, the energy difference is even more extreme.

B2e. Summary

In summary, the adspecies of metal alkyl molecules on chemically passivated silicon surfaces have been studied by using infrared total-internal reflection as well as ultraviolet transmission. These submonolayer-sensitive techniques allow us to investigate the surface photophysics of chemisorbed layers. In addition, temperature-programmed-desorption spectroscopy and mass spectroscopy of laser-induced desorption were used to determine the identity of the chemisorbed species and their fragments under ultraviolet photodissociation. It has been shown that these molecules chemisorbed intact on surface hydroxyl groups with ~1.1-eV binding energy. Their photodecomposition is strongly wavelength dependent since the methyl dissociation fragment is observed at 193 nm whereas no fragments from the surface can be detected for 248 nm. The roles of both the adspecies-substrate interaction and the gas-phase photodissociation processes are believed to be responsible for this effect.

B3. Laser Photodeposition of Cd for the Fabrication of Elevated Barrier Height Schottky Diodes

As a demonstration of our ability to manipulate monolayers of the above organometallics and to compare the surface chemistry of these molecules on more reactive surfaces, we have studied the reactions of these divalent metal alkyls on bare semiconducting surfaces. This study also had an important side benefit. One of the intents of the work reported below was to form (using laser photodeposition), evaluate and utilize Cd/*n*-semiconductor junction. As Cd is a *p*-type dopant in InP and $In_{0.53}Ga_{0.47}As$, indiscriminant laser heating during the deposition process could produce unintentional doping and the formation of *p*/*n* junctions enhanced diodes. In order to choose deposition fluences low enough to avoid significant surface heating, numerical calculations of the laser-induced temperature rises as a function of incident power were performed before deposition.[88] In these calculations, the thermal conductivities, specific heats and fundamental energy band gaps were taken into account as functions of temperature. On the other hand, the absorption constants and reflectivities were assumed to be independent of temperature, but fixed for the specific excimer wavelength used. The calculated temperature rise as a function of incident power for 248-nm excimer irradiation at 10 Hz is shown in Figure 24 for InP and $In_{0.53}Ga_{0.47}As$ substrates. The low power density of 3 mJ/cm^2 used in our experiments is expected to produce a peak temperature rise of only 18 °C on InP substrates. The expected peak rise on $In_{0.53}Ga_{0.47}As$ substrates is 56 °C due to the fact that the thermal conductivity of $In_{0.53}Ga_{0.47}As$ is roughly three times lower than that of InP. The steady-state temperature rises are expected to be sensitive to the sample mounting procedure. In this case,

[88] T.J. Licata, *Ph.D. dissertation (Columbia University, New York, 1990).*

the samples had blanket ohmic back contacts and were attached to a 20-cm^3 Al mounting block using silver paint. Thus, very good thermal contact was established and the laser heating was diffused throughout the entire thermal mass on a time scale of ~1 s. Based on a solution of the heat equation,[89] the estimated steady-state temperature rise after 2000 pulses is between 0.10 and 0.25 °C, assuming the entire thermal mass to be either Al or InP. Such heating is inconsequential for our experiments.

B3a. Excimer-Photodeposited Cd on InP and $In_{0.53}Ga_{0.47}As$

Efforts to elevate the Schottky barrier heights to semiconductors, and InP and$In_{0.53}Ga_{0.47}As$ in particular, have generally been based on interposing a high band gap layer or a *p-n* junction between a metal contact layer and the semiconductors.[90,91,92,93,94,95,96,97,98,99] However,

---

[89] C. Kittel and H. Kroemer, *Thermal Physics, p. 427 (Freeman, New York, 1980).*

[90] T.Y. Chang, R.F. Leheny, R.E. Nahory, E. Silberg, A.A. Ballman, E.A. Caridi and C.J. Harrold, *IEEE Electron Device Lett. EDL-3, 56 (1982).*

[91] K. Steiner, U. Seiler and K. Heime, *Appl. Phys. Lett. 53, 2513 (1988).*

[92] O. Wada and A. Majerfeld, *Electron. Lett. 14, 125 (1978).*

[93] D.V. Morgan and J. Frey, *Electron. Lett. 14, 737 (1978).*

[94] H. Morkoc, T.J. Drummond and C.M. Stanchak, *IEEE Trans. Electron. Dev. ED-28, 1 (1981).*

[95] P.D. Gardner, S.G. Liu, S.Y. Narayan, S.D. Colvin, J.P. Paczkowski and D.R. Capewell, *IEEE Electron. Device Lett. EDL-7, 363 (1986).*

[96] S. Loualiche, H. L'Haridon, A. Le Corre, D. Lecrosnier, M. Salvi and P.N. Favennec, *Appl. Phys. Lett. 52, 540 (1988).*

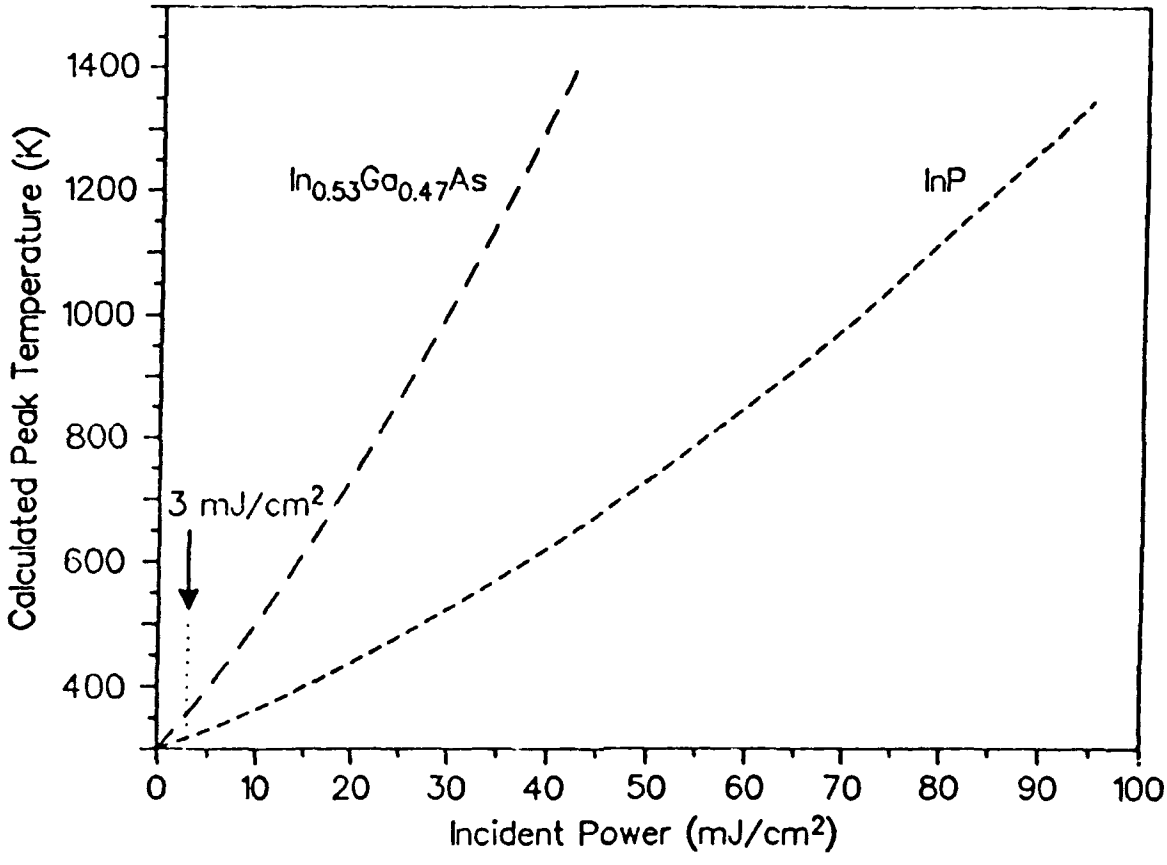

Figure 24 Calculated peak temperature rises for InP and $In_{0.53}Ga_{0.47}As$ substrates irradiated with 23-ns long pulses of 248-nm photons from an KrF excimer laser.

recent work has demonstrated that there are metals that exhibit intrinsically high barrier heights with InP. Specifically, Sa and Meiners found barrier heights of 0.62 eV and 0.92 eV for electroplated cadmium and mercury point contacts with InP.[100] Electroplated cadmium-based metal-semiconductor field effect transistors (MESFETs) were soon fabricated, albeit with 100-μm gate lengths.[101] As electroplating of Cd is not well-suited to forming micrometer-scale device structures, and evaporation of uniform Cd layers is difficult, alternative deposition techniques for Cd films are drawing new attention.[102,103]

Here, we present a single-step, potentially metallorganic chemical vapor deposition (MOCVD) and metallorganic molecular beam epitaxy (MOMBE) -compatible method for the fabrication of Cd/InP and Cd/$In_{0.53}Ga_{0.47}As$ interfaces and demonstrate its applicability to the formation of micrometer-scale electronic devices. Specifically, a thin Cd layer is photodeposited on the semiconductor surface prior to evaporation of a thicker Au contact layer. In this technique, which has been described in detail elsewhere,[104] low power ultraviolet photons irradiate the sample in a dimethyl cadmium (DMCd) ambient. Dissociation of the gas and surface phase DMCd molecules occurs through a purely photolytic mechanism. Note that in all the experiments reported here, laser heating of the semiconductor surface was sufficiently small

---

100 C.J. Sa and L.G. Meiners, *Appl. Phys. Lett. 48, 1796 (1986).*

101 L.G. Meiners, A.R. Clawson and R. Nguyen, *Appl. Phys. Lett. 49, 340 (1986).*

102 W.K. Chan, H.M. Cox, J.H. Abeles, S.P. Kelty, *Electron. Lett. 23, 1346 (1987).*

103 W.K. Chan, G. Chang, R. Bhat and N.E. Schlotter, *IEEE Electron. Device Lett. EDL-9, 220 (1988).*

104 T.J. Licata, M.T. Schmidt, D.V. Podlesnik, V. Liberman, R.M. Osgood, Jr., W.K. Chan and R. Bhat, *J. Electron. Mater. 16, 1239 (1990).*

to preclude pyrolytic dissociation of DMCd or diffusion of Cd into the semiconductor.[104] We have applied the photodeposition process to the formation of Schottky barrier diodes on InP and $In_{0.53}Ga_{0.47}As$ and $In_{0.53}Ga_{0.47}As$ MESFETs. For the Schottky diodes, a non-lithographic, shadow-mask process was used to fabricate large-area (0.015 cm^2) Au/InP, Au/Cd/InP, $Au/In_{0.53}Ga_{0.47}As$ and $Au/Cd/In_{0.53}Ga_{0.47}As$ contacts for determination of the Schottky barrier heights through current-voltage (I-V) measurements. Blanket AuGeNi ohmic back contacts were formed on bulk $5x10^{17}$ cm^{-3} Te-doped semiconductor samples. The samples were degreased and then deoxidized for one minute using an NH_4OH/H_2O solution (1:1 for InP, 1:10 for $In_{0.53}Ga_{0.47}As$).[105] The samples were then loaded within two minutes into a cryopumped stainless steel high-vacuum cell having a base pressure of $1x10^{-7}$ Torr. For Cd depositions, the vacuum cell was statically-filled to 1 Torr of DMCd. The λ=248 nm beam of a KrF excimer laser was attenuated to 3 mJ/cm^2 per pulse. Blanket depositions of Cd were accomplished using 2,000 laser pulses (10 Hz for 200 seconds), which resulted in the formation of visible Cd films on the samples and cell window. Based on Auger electron spectroscopy depth profiling of our Cd films, we estimate a thickness of ~200 Å. After a two-minute exposure to air during transit, the Cd-coated samples were mounted next to control samples in a conventional thermal evaporator. A 1,500-Å thick Au film was evaporated through a Mo shadow mask to form the diode structures. Before I-V measurements, all samples were submerged in 25% HCl for two minutes to etch away all exposed Cd, since failure to do this resulted in large short-circuit currents carried by the Cd blanket film to the ohmic back contact. Control samples not coated with Cd showed no such shorting. The Schottky barrier heights and ideality factors (n) were

---

105 D.E. Aspnes and A.A. Studna, *Appl. Phys. Lett. 39, 316 (1981).*

obtained from I-V characteristics. The values of ϕ_b determined from these experiments are 0.70 eV for Au/Cd/InP (n=1.03) and 0.55 eV for Au/Cd/$In_{0.53}Ga_{0.47}As$ (n=1.08). These barrier heights are significantly higher than the barrier heights formed between Au and InP or $In_{0.53}Ga_{0.47}As$ (0.43 eV[106] and 0.25 eV,[107] respectively), thereby making fabrication of FETs on both substrates feasible. As a demonstration of the applicability of this process to the fabrication of micrometer-scale devices, *n*-channel depletion-mode $In_{0.53}Ga_{0.47}As$ field-effect transistors with Au/Cd gates were fabricated using conventional photolithographic techniques. MOCVD was used to grow the various epitaxial layers on a semi-insulating InP substrate. A 2,500-Å thick, $6x10^{16}$ cm^{-3} Te-doped $In_{0.53}Ga_{0.47}As$ channel was chosen to provide a high transconductance and a low pinch-off voltage, whereas the 1,000-Å thick, $6x10^{18}$ cm^{-3} Te-doped cap layer was used to facilitate formation of the ohmic contacts. Isolation mesas to the InP substrate were formed by Ar-ion milling followed by a one minute etch in H_3PO_4:H_2O_2:H_2O (1:1:38). AuGeNi ohmic contacts were used for the source and drain contacts. The source resistance was measured to be 1.06 Ω-mm. Photoresist was patterned with openings for the 1.2-μm long gates. The photoresist served as a mask both for the gate recess etch and for the subsequent gate metal liftoff. After the gate recess etch, the samples were deoxidized in dilute NH_4OH, and loaded into the Cd deposition cell. After Cd deposition, as above, and evaporation of a Au blanket film, a lift-off in acetone was used to define the 1.2-μm gate. We note that the photodeposition process produced a uniform Cd layer over the ~1 cm^2 samples used in these

---

106 N. Newman, T. Kendelewicz, L. Bowman and W.E. Spicer, *Appl. Phys. Lett. 46, 1176 (1985).*

107 K. Kajiyama, Y. Mizushima and S. Sakata, *Appl. Phys. Lett. 23, 458 (1973).*

experiments and did not limit the device yield.

B3b. XPS Characterisation of Excimer-Photodeposited Cd on InP and $In_{0.47}Ga_{0.53}As$

One of the issues which has limited widespread use of InP and $In_{0.47}Ga_{0.53}As$ for electronic device applications is the low Schottky barrier for most metals on these semiconductors. Above, we reported that 248-nm excimer laser photodeposited Cd from dimethylcadmium (DMCd) forms relatively high barriers to these semiconductors (0.70 eV and 0.55 eV, respectively).[104] Furthermore, we integrated the photodeposition process with conventional lithographic processing to fabricate high speed (30 GHz), high transconductance (200 mS/mm), 1.2-μm gate length Au/Cd/$In_{0.47}Ga_{0.53}As$ MESFETs.[104] Below, we report the use of X-ray photoemission spectroscopy to investigate the interfacial chemistry characteristic and spectroscopy of Cd/InP and Cd/$In_{0.47}Ga_{0.53}As$ interfaces formed through *in situ* processing. Specifically, we report on the spontaneous interactions upon room temperature DMCd adsorption on surfaces prepared using different procedures. In addition, we investigate the effect of photodeposition on the interfacial layer. Saturation exposure of clean surfaces to DMCd results in dissociative chemisorption to yield some metallic Cd, some alkylated Cd and a reacted Cd compound. Photodeposition of several additional Cd monolayers increases the amount of substrate-reacted Cd. After the reacted compound reaches a self-limiting thickness, further deposition results in a metallic Cd layer. X-ray photoemission spectroscopy analysis was used to investigate *in situ* prepared Cd/InP interfaces. In these experiments, a monochromatized Al Kα line (1486.6 eV) was used to monitor the In and Cd $3d_{5/2}$ peaks, the C and O 1s peaks, and the P 2p peak. Exposure of chemically cleaned surfaces to the standard deposition ambient of

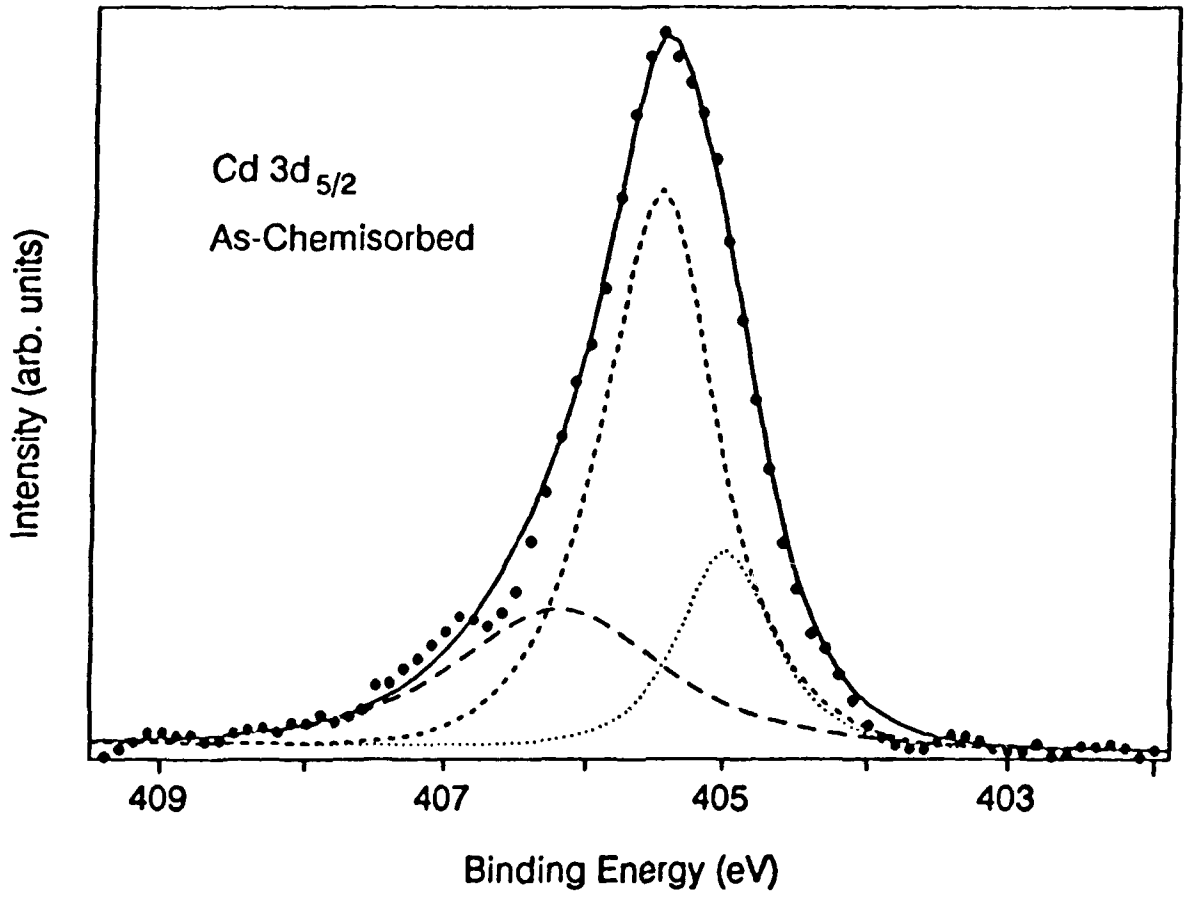

Figure 25 Monochromatic Al X-ray photoelectron spectroscopy $Cd_{5/2}$ peak for chemically-cleaned InP exposed to 1 Torr of DMCd for 5 minutes with no irradiation (as-chemisorbed). The peak was fitted to three components corresponding to the metallic Cd (405.0 eV), monomethyl cadmium (405.5 eV) and a peak at 406.0 eV due to a spontaneous formed interfacial compound.

1 Torr DMCd for five minutes without irradiation produced a slight elevation of the C peak and the appearance of the broad, slightly asymmetric Cd peak shown in Figure 25. Due to the peak's breadth and previous work,[63] we used three components to fit this feature. The lowest binding energy component (405.0 eV) corresponds to metallic Cd, whereas the higher binding energy components correspond to reacted Cd species. Note that in all our data analysis, the 0.5 eV peak separations were kept constant. The absolute positions of the peaks, however, were allowed to move in order to account for Fermi level shifts and matrix effects. Although the peaks at 405.5 and 406.0 eV have been attributed to an adsorbed layer of partially and undissociated DMCd on other substrates,[63] changes in the peak areas after heat treatment and as a function of the amount of deposited Cd[104] argue that for DMCd on InP, these peaks correspond to reacted Cd compounds. In one such experiment, ~30 Å of Cd was photodeposited on a chemically cleaned surface (Figure 26) which was then heated to 300°C in vacuum for 5 minutes (Figure 27). Figure 27 shows that the heat treatment caused the high energy peaks from reacted Cd to increase at the expense of the metallic Cd peak under conditions where no physisorption of DMCd was possible. Note that the high energy side of the as-deposited spectrum (Figure 26) was fitted using only one component, since the attenuated high energy peaks from the buried reacted layer were too weak to fit unambiguously with two components. Separate experiments on ultra-high-vacuum-prepared surfaces indicate that the component at 405.5 eV corresponds to a Cd-P compound, and the component at 406.0 eV corresponds to oxidized Cd. Thus, dark adsorption of DMCd onto chemically cleaned InP results in spontaneous dissociation of the DMCd to form metallic Cd, a Cd-P compound (from reaction with the substrate) and a Cd-O compound (from reaction with the monolayer-scale native oxide). After the reacted

interfacial layer has formed, photodeposition of Cd produces a clean metallic layer with no elevation of C over the as-chemisorbed levels. Attenuation of substrate peaks and reacted Cd peaks as a function of the amount of Cd photodeposited on the surface shows that the extent of the spontaneously formed reacted layer and any associated disruption of the interface is only ~10 Å or so at room temperature. Our measurements of In and P core level spectra did not allow us to determine the stoichiometry of the substrate-reacted Cd compound. However, based on the lack of a measurable shift in our In peak (which would indicate segregated In), and thermodynamic considerations,[104] we believe the interfacial compound to be a $Cd_xIn_yP_z$ compound.

C. Scientific Personnel Supported and Degrees Awarded

Graduate Students

Bertrand Quiniou Ph.D. 1992

Research Scientists

Jianhua Wang

Ken Miyano

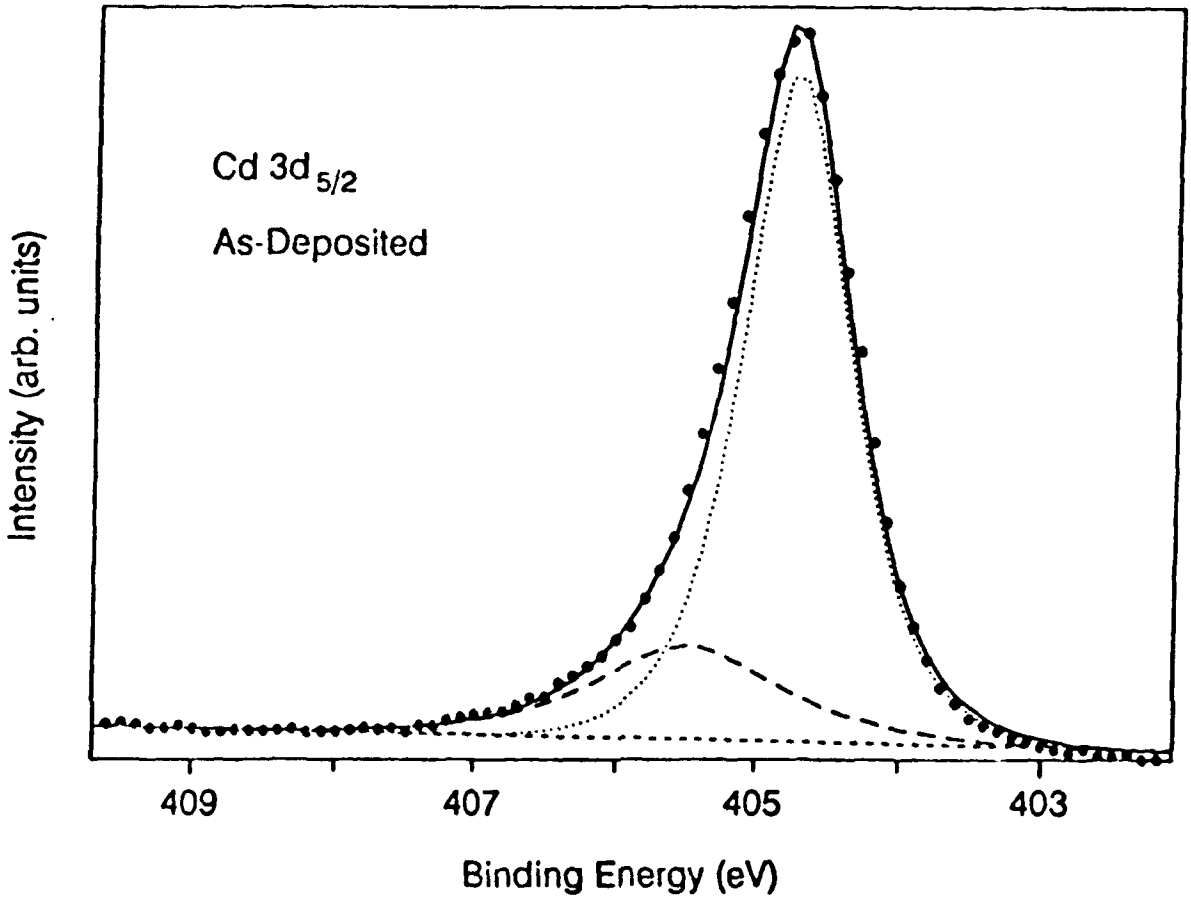

Figure 26 X-ray photoelectron spectroscopy $Cd_{5/2}$ peak for photodeposited Cd. No thermal treatment was applied to the sample after photodeposition.

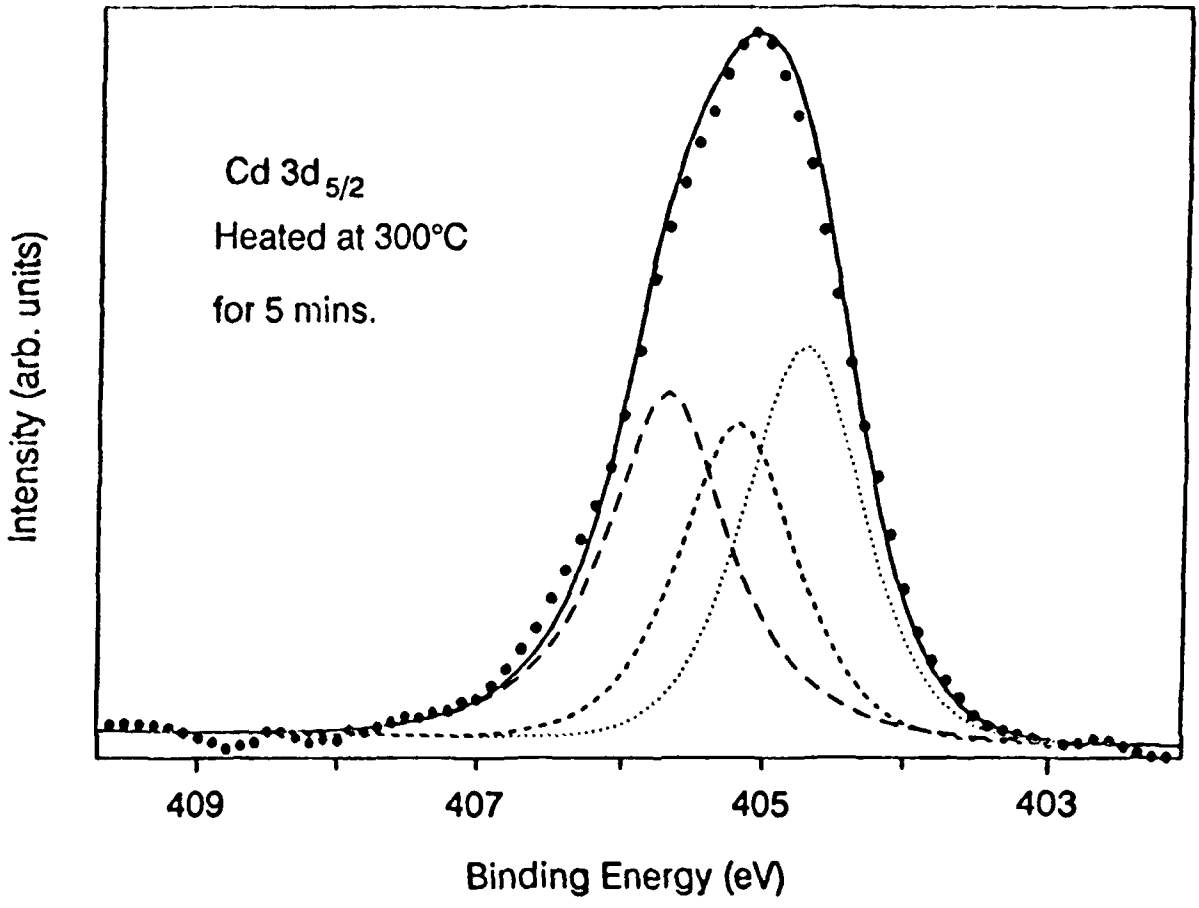

Figure 27 X-ray photoelectron spectroscopy Cd $3d_{5/2}$ peak for 30 Å of photodeposited Cd, after heating of the sample to 300 °C in vacuum for 5 minutes. Upon heating, the peak at 406 eV increased at the expense of the peak at 405.0 eV. Note that desorption of Cd upon heating resulted in a drop in the measured Cd 3d intensity before normalization to yield this plot. However, the absolute intensity of the peak at 406 eV increased by ~50%.

Significant Papers Published or Submitted Under Existing ARO Program

1. J. A. O'Neill, E. Sanchez and R. M. Osgood Jr., "Infrared Internal Reflection Studies of the Surface Photochemistry of Dimethylcadmium on Silicon," Journal of Vacuum Science and Technology A7 3, 2110 (1989).

2. P. Shaw, J. A. O'Neill, E. Sanchez, Z. Wu and R. M. Osgood Jr., "The Spectroscopy and Surface Chemistry of Metal-Alkyl Molecules," Materials Research Society Proceedings, 129, 45 (1989).

4. P. S. Shaw, E. Sanchez, J. A. O'Neill, Z. Wu and R. M. Osgood, Jr. "Surface Photochemistry of Divalent Metal Alkyls on SiO(2)," Journal of Chemical Physics Letters 94, 1634 (1991).

5. R. M. Osgood Jr., "Laser-Fabrication for Solid-State Electronics," IEEE Circuits and Devices Magazine (September, 1990), p. 25.

6. R. M. Osgood Jr., "Laser-Fabrication for Integrated Electronics and Optics," OITDA Conference, Tokyo, Japan, July 5-6, 1990.

7. M. Ruberto, X. Zhang, R. Scarmozzino, A. Willner, D. V. Podlesnik and R. M. Osgood Jr., "The Laser-Controlled Micrometer-Scale Photoelectrochemical Etching of III-V Semiconductors," Journal of the Electrochemical Society 138, 1174 (1991).

8. B. Quiniou, W. Schwarz, Z. Wu and R. M. Osgood Jr., "Photoemission from Thick Overlying Epitaxial Layers of CaF(2) on Si(111)," Appl. Phys. Lett. 60, 183 (1992).

9. Z. Wu, B. Quiniou, J. Wang and R. M. Osgood Jr., "Temperature and Adsorbate Dependence of the Image-Potential States on Cu(100)," accepted for publication in Phys. Rev. B (1992).

Presentations to Industry and Symposia

1. IBM, Yorktown Heights, NY, March 13, 1989
   "The Surface Spectroscopic Study of Organometallic Molecules," Ping S. Shaw

2. MAX-PLANCK-INSTITUT fur BIOPHYSIKALISCHE CHEMIE, Schloss Ringberg, June 12, 1989, Laser Induced Surface Modification, "Laser Induced Chemical Surface Modification," Richard M. Osgood, Jr.

3. DIGITAL, Shrewsbury, MA, October 10, 1989
   Laser Processing Seminar, "Advanced Photon Processing for VLSI," Richard M. Osgood, Jr.

4. AMERICAN CHEMICAL SOCIETY MEETING, Miami, FL, September 13, 1989
   Symposium on Surface Photochemistry, "Photochemistry of Surface-Bound Metal Alkyls," Richard M. Osgood, Jr.

5. IBM, T.J. Watson Research Laboratories, Yorktown Heights, NY, September 29, 1989
   Short Course, "Laser Chemical Processing - A Tutorial Overview," Richard M. Osgood, Jr.

6. ISPSR Conference, Kyoto, Japan, November 14, 1989
   "Laser Surface Chemistry for Microelectronics," Richard M. Osgood, Jr.

7. IBM, T. J. Watson Research Lab., Yorktown Heights, NY, January 8, 1990
   "Fundamental Mechanisms in UV-Assisted Surface Reactions," Richard M. Osgood, Jr.

8. CITY UNIVERSITY OF NEW YORK, New York, NY, September 12, 1990
   "The Chemical Physics of Light-Surface Interactions," Richard M. Osgood, Jr.

9. MICROPHYSICS OF SURFACES CONFERENCE, Sante Fe, New Mexico, February 11-13, 1991, "Photoemission from Si(111) Surfaces Covered with Thick Overlayers of CaF(2)," Bertrand Quiniou

10. AMERICAN PHYSICAL SOCIETY, Washington, DC, April 22-25, 1991
    "Temperature and Adsorbate Dependence of Image Potential States on Cu(100)," Bertrand Quiniou

11. IBM, Almaden, CA, January, 1992
    "Laser Photoelectron Spectroscopy," Richard M. Osgood, Jr.